# Highly improved staggered quarks on the lattice with applications to charm physics

E. Follana,[1,*] Q. Mason,[2] C. Davies,[1] K. Hornbostel,[3] G. P. Lepage,[4] J. Shigemitsu,[5] H. Trottier,[6] and K. Wong[1]

[1]*Department of Physics and Astronomy, University of Glasgow, Glasgow, United Kingdom*
[2]*Department Applied Maths and Theoretical Physics, Cambridge University, Cambridge, United Kingdom*
[3]*Southern Methodist University, Dallas, Texas 75275, USA*
[4]*Laboratory for Elementary-Particle Physics, Cornell University, Ithaca, New York 14853, USA*
[5]*Physics Department, The Ohio State University, Columbus, Ohio 43210, USA*
[6]*Physics Department, Simon Fraser University, Vancouver, British Columbia, Canada*

(Received 15 October 2006; published 14 March 2007)

We use perturbative Symanzik improvement to create a new staggered-quark action (HISQ) that has greatly reduced one-loop taste-exchange errors, no tree-level order $a^2$ errors, and no tree-level order $(am)^4$ errors to leading order in the quark's velocity $v/c$. We demonstrate with simulations that the resulting action has taste-exchange interactions that are 3–4 times smaller than the widely used ASQTAD action. We show how to bound errors due to taste exchange by comparing ASQTAD and HISQ simulations, and demonstrate with simulations that such errors are likely no more than 1% when HISQ is used for light quarks at lattice spacings of $1/10$ fm or less. The suppression of $(am)^4$ errors also makes HISQ the most accurate discretization currently available for simulating $c$ quarks. We demonstrate this in a new analysis of the $\psi - \eta_c$ mass splitting using the HISQ action on lattices where $am_c = 0.43$ and 0.66, with full-QCD gluon configurations (from MILC). We obtain a result of 111(5) MeV which compares well with the experiment. We discuss applications of this formalism to $D$ physics and present our first high-precision results for $D_s$ mesons.

DOI: 10.1103/PhysRevD.75.054502 PACS numbers: 11.15.Ha, 12.38.Aw, 12.38.Gc

## I. INTRODUCTION

The reintroduction of the staggered-quark discretization in recent years has transformed lattice quantum chromodynamics, making accurate calculations of a wide variety of important nonperturbative quantities possible for the first time in the history of the strong interaction [1–5]. Staggered quarks were introduced 30 years ago, but unusually large discretization errors, proportional to $a^2$ where $a$ is the lattice spacing, made them useless for accurate simulations. It was only in the late 1990s that we discovered how to remove the leading errors, and the result was one of the most accurate discretizations in use today. Staggered quarks are faster to simulate than other discretizations, and as a result have allowed us for the first time to incorporate (nearly) realistic light-quark vacuum polarization into our simulations. This makes high-precision simulations, with errors of order a few percent, possible for the first time (see [1] for a more detailed discussion). In this paper we present a new discretization that is substantially more accurate than the improved discretization currently in use. With this new formalism accurate simulations will be possible at even larger lattice spacings, further reducing simulation costs.

The $\mathcal{O}(a^2)$ discretization errors in staggered quarks have two sources. One is the usual error associated with discretizing the derivatives in the quark action. The correction for this error is standard and was known in the 1980s [6]. The second source was missed for almost a decade. It results from an unusual property of the staggered-quark discretization: the lattice quark field creates four identical flavors or tastes of quark rather than one. (We refer to these unphysical flavors as ''tastes'' to avoid confusion with the usual quark flavors, which are not identical since quarks of different flavor have different masses.) The missing $a^2$ error was associated with taste-exchange interactions, where taste is transferred from one quark line to another in quark-quark scattering. The generic correction for this type of error involves adding four-quark operators to the discretized action.

Taste is unphysical. Instead of one $\pi^+$, for example, one has 16. Taste is easily removed in simulations provided that different tastes are exactly equivalent, which they are, and provided there are no interactions that mix hadrons of different taste. Taste-exchange interactions, however, cause such mixing, and therefore it is crucial that we understand such interactions and suppress them. Furthermore, past experience suggests that the errors due to residual taste exchange are the largest remaining $a^2$ errors in current simulations.

The corrections to the lattice action that suppress taste exchange were missed initially because four-quark operators are not usually needed to correct discretization errors in lowest order perturbation theory (that is, at tree level). They were first discovered empirically from simulations in which the gluon fields in the quark action were replaced by smeared fields, which happen to suppress taste-changing quark-quark scattering amplitudes [7]. This discovery led to a proper understanding of the taste-exchange mechanism [8,9], and to the first correct analysis of the $a^2$ errors in staggered-quark formalisms [8,10]. The resulting ''ASQTAD'' quark action has provided the basis for almost

*Electronic address: e.follana@physics.gla.ac.uk

 

all simulations to date that include (nearly) realistic light-quark vacuum polarization.

While it is possible to remove all tree-level taste exchange by smearing the gluon fields appropriately, higher-order corrections can only be removed by adding four-quark operators. Recent numerical experiments suggest, however, that even these corrections can be significantly suppressed through additional smearing [11]. These studies, while very important, were limited in two ways. First, they used the mass splittings between the 16 tastes of pion as a probe for taste exchange; there are many taste-exchange interactions that do not affect this spectrum. Second, smearing the gluon fields introduces other types of $\mathcal{O}(a^2)$ error which undo the advantage of an improved discretization (that is, accuracy at large values of $a$).

In this paper we present the first rigorous analysis of one-loop taste exchange. Based upon this analysis we develop a simple smearing scheme that suppresses one-loop corrections by an order of magnitude on average. Our smearing scheme is simpler than that in [11] and, unlike that scheme, it does not introduce new $a^2$ errors. The result is a new discretization for highly improved staggered quarks which we refer to by the acronym HISQ.

An added advantage of a highly improved action is that it can be used to simulate $c$ quarks. Heavy quarks are difficult to simulate using standard discretizations because discretization errors are large unless $am \ll 1$, where $a$ is the lattice spacing and $m$ the quark mass. To simulate $b$ quarks, for example, one would require lattice spacings substantially smaller than $1/20$ fm—much too small to be practical today. Consequently high-quality simulations of $b$ quarks rely upon rigorously defined effective field theories, like nonrelativistic QCD [12], that remove the rest mass from the quark's energy. While this approach works very well for $b$ quarks, it is less successful for $c$ quarks because the quark's mass is much smaller, and consequently $c$ quarks are much less nonrelativistic. The smaller quark mass, however, means that $am_c \approx 1/2$ for lattice spacings of order $1/10$ fm, which are typical of simulations today. As we demonstrate in this paper, we can obtain few-percent accuracy for charm quarks when $am_c \approx 1/2$ provided we use a highly improved relativistic discretization like HISQ.

In Sec. II we review the (perturbative) origins of taste-exchange interactions in staggered quarks, and their removal at lowest order (tree level) in perturbation theory, using the Symanzik improvement procedure. We also extend the traditional Symanzik analysis to cancel all $(am)^4$ errors to leading order in the quark's velocity, $v/c$ (in units of the speed of light $c$). The additional correction needed is negligible for light quarks, but significantly enhances the precision of $c$-quark simulations.

In Sec. III, we extend our analysis of taste exchange to one-loop order, and show how to suppress such contributions by approximately an order of magnitude, thereby effectively removing one-loop taste exchange from the theory. The resulting quark action (HISQ) is the first staggered-quark discretization that is both free of lattice artifacts through $\mathcal{O}(a^2)$ and effectively free of all taste exchange through one-loop order. We also identify the order $\alpha_s(am)^2$ corrections to the action that are important for high-precision $c$ physics.

We illustrate the utility of our new formalism, in Sec. IV, first by examining its effect on taste splittings in the pion spectrum. We also show how to directly bound the size of taste-exchange interactions in simulations by comparing ASQTAD and HISQ simulations at the same lattice spacing. There has been much discussion recently about the formal problems caused by taste exchange [13]. The issues are summarized by Sharpe in [14]. His conclusion, with which we agree, is that the errors associated with taste exchange vanish in the continuum limit. His formal analysis gives no indication, however, of the size of these errors for the finite lattice spacings in current use. Assuming that taste-exchange errors vanish in the continuum limit, the differences between ASQTAD and HISQ measurements at any lattice spacing can be used to bound the taste-exchange errors in each measurement since taste-exchange errors will be much smaller in HISQ.

We report on a new simulation of $c$ quarks and charmonium using the HISQ formalism in Sec. V. This is the most severe test of the HISQ formalism since $am_c \approx 1/2$ for the lattice spacings we use, but we show that the formalism delivers results that are accurate to a couple of percent, making it the most accurate formalism available for simulating $c$ quarks. We demonstrate this in a new high-precision determination of the $\psi - \eta_c$ splitting. This analysis confirms our expectation that the largest $a^2$ errors in the ASQTAD action are associated with taste exchange, and we show that these are greatly reduced by using the HISQ action instead.

The moderately heavy smearing used in the HISQ formalism complicates unquenched simulations. In Sec. VI, we discuss how these complications can be dealt with. Finally, in Sec. VII, we summarize our results and discuss their relevance to future work. Here we also present our first $D$ physics results from the HISQ action.

Much of our discussion is framed in terms of the "naive" discretization for quarks, which is conceptually equivalent to the staggered-quark discretization (see Appendix B). We usually find naive quarks to be more intuitive in analytic work than staggered quarks, while the latter formalism is definitely the more useful one for numerical work. We outline the formal connection between the naive-quark and staggered-quark formalisms in a series of detailed appendices. We use these results in our one-loop analysis of taste-exchange interactions, which is described in detail in Appendix F.

It is also clear, using naive quarks, that there can be no $\mathcal{O}(a)$ errors of any sort in these formalisms. This appears to

TABLE I. Gluon configurations used in this paper with information about the collaboration that produced them, the lattice spacing $a$, the gluon action used (the unimproved quenched Wilson action or the Symanzik-improved Lüscher-Weisz action for full $n_f = 3$ QCD), the $s$ and $u = d$ quark masses used in vacuum polarization (here $u_0$ is the fourth root of the gluon plaquette operator), and the spatial size of the lattice. The first set of configurations is described in [15], while the others are discussed in detail in [1,16].

| | $a$ (fm) | Gluon action | $u_0 am_s$ | $u_0 am_{u/d}$ | $L/a$ |
|---|---|---|---|---|---|
| UKQCD | 1/10 | Wilson | — | — | 16 |
| MILC | 1/8 | Lüscher-Weisz | 0.05 | 0.01 | 20 |
| MILC | 1/11 | Lüscher-Weisz | 0.03 | 0.006 | 28 |

contradict some older treatments of staggered quarks, which find taste-exchange errors in $\mathcal{O}(a)$ even for free quarks. At the end of Appendix C, we discuss why these $\mathcal{O}(a)$ effects are artifacts of the particular way in which these older treatments isolate different tastes; the artifacts have nothing to do with the underlying theory and do not affect physical quantities.

We used several sets of gluon configurations in this paper. The parameters for these various sets are summarized in Table I.

## II. SYMANZIK IMPROVEMENT FOR NAIVE/STAGGERED QUARKS

### A. Naive quarks, doubling, and taste-changing interactions

We begin our review of staggered quarks by examining the formally equivalent naive discretization of the quark action (see Appendix B):

$$\mathcal{S} = \sum_x \bar{\psi}(x)(\gamma \cdot \Delta(U) + m_0)\psi(x), \tag{1}$$

where $\Delta_\mu$ is a discrete version of the covariant derivative,

$$\Delta_\mu(U)\psi(x) \equiv \frac{1}{2a}(U_\mu(x)\psi(x + a\hat{\mu}) - U_\mu^\dagger(x - \hat{\mu})\psi(x - a\hat{\mu})), \tag{2}$$

$U_\mu(x)$ is the gluon link-field, $a$ the lattice spacing, and $m_0$ is the bare quark mass. The gamma matrices are Hermitian, with

$$\gamma_\mu^\dagger = \gamma_\mu, \qquad \gamma_\mu^2 = 1, \qquad \{\gamma_\mu, \gamma_\nu\} = 2\delta_{\mu\nu}, \tag{3}$$

where indices $\mu$ and $\nu$ run over $0 \ldots 3$. A complete set of 16 spinor matrices can be labeled by four-component vectors $n_\mu$ consisting of 0s and 1s (i.e., $n_\mu \in \mathbb{Z}_2$):

$$\gamma_n \equiv \prod_{\mu=0}^{3} (\gamma_\mu)^{n_\mu}. \tag{4}$$

A set of useful gamma-matrix properties is presented in Appendix A.

The naive-quark action has an exact "doubling" symmetry under the transformation:

$$\psi(x) \to \tilde{\psi}(x) \equiv \gamma_5\gamma_\rho(-1)^{x_\rho/a}\psi(x) = \gamma_5\gamma_\rho \exp(ix_\rho\pi/a)\psi(x). \tag{5}$$

Thus any low energy-momentum mode, $\psi(x)$, of the theory is equivalent to another mode, $\tilde{\psi}(x)$, that has momentum $p_\rho \approx \pi/a$, the maximum allowed on the lattice. This new mode is one of the "doublers" of the naive-quark action. The doubling transformation can be applied successively in two or more directions; the general transformation is

$$\psi(x) \to \mathcal{B}_\zeta(x)\psi(x), \qquad \bar{\psi}(x) \to \bar{\psi}(x)\mathcal{B}_\zeta^\dagger(x), \tag{6}$$

where

$$\mathcal{B}_\zeta(x) \equiv \gamma_{\bar{\zeta}}(-1)^{\zeta\cdot x/a} \propto \prod_\rho (\gamma_5\gamma_\rho)^{\zeta_\rho} \exp(ix \cdot \zeta\pi/a), \tag{7}$$

and $\zeta$ is a vector with $\zeta_\mu \in \mathbb{Z}_2$, while $\bar{\zeta}$ is "conjugate" to $\zeta$ (see Appendix A):

$$\bar{\zeta}_\mu \equiv \sum_{\nu\neq\mu} \zeta_\nu \bmod 2. \tag{8}$$

Consequently there are 15 doublers in all (in four dimensions), which we label with the 15 different nonzero $\zeta$'s.

As a consequence of the doubling symmetry, the standard low-energy mode and the 15 doubler modes must be interpreted as 16 equivalent flavors or tastes of quark. (The 16 tastes are reduced to four by staggering the quark field; see Appendix B.) This unusual implementation of quark tastes has surprising consequences. Most striking is that a low-energy quark that absorbs momentum close to $\zeta\pi/a$, for one of the 15 $\zeta$'s, is not driven far off energy-shell. Rather it is turned into a low-energy quark of another taste. Thus the simplest process by which a quark changes taste is the emission of a single gluon with momentum $q \approx \zeta\pi/a$. This gluon is highly virtual, and therefore it must immediately be reabsorbed by another quark, whose taste will also change (see Fig. 1).

Taste exchange necessarily involves highly virtual gluons. This means that taste exchange is perturbative for typical lattice spacings. It also means that it is suppressed by $a^2$: the effect of the process in Fig. 1 is indistinguishable from that of a local four-quark operator when the gluon is highly virtual, and four-quark operators, being dimension six, are suppressed by $(pa)^2$ where $p$ is a typical external momentum. One-gluon exchange, with gluon momentum $q \approx \zeta\pi/a$, is the dominant flavor-changing interaction since it is lowest order in $\alpha_s(\zeta\pi/a)$ and involves only 4 external quark lines. (Processes with more quark lines are suppressed by additional powers of $(ap)^3$.) This observation is crucial when trying to improve naive quarks by

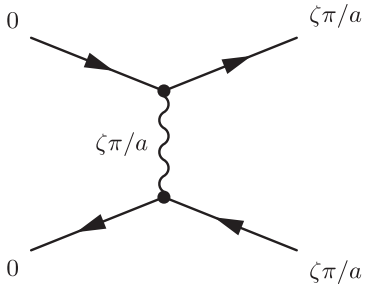


FIG. 1. The leading tree-level taste-exchange interaction, which involves the exchange of a gluon with momentum $\zeta\pi/a$ where each $\zeta_\mu$ is 0 or 1 but $\zeta^2 \neq 0$.

removing finite-$a$ errors, as we discuss below (see also [8–10]).

Sixteen tastes of quark from a single quark field is 15 too many. Ignoring taste exchange for the moment, factors of $1/16$ are easily inserted into simulations to remove the extra copies. In particular, quark vacuum polarization is corrected by replacing the quark determinant in the path integral by its $1/16$ root,

$$\det(\gamma \cdot \Delta + m_0) \rightarrow \det(\gamma \cdot \Delta + m_0)^{1/16}, \tag{9}$$

or, equivalently, by multiplying the contribution from each quark loop by $1/16$. This works because, absent taste exchange, the naive-quark Dirac operator has in effect a $16 \times 16$ block-diagonal matrix structure,

$$\Delta \cdot \gamma + m_0 \sim \begin{pmatrix} \mathcal{D}(U) & 0 & \cdots & 0 \\ 0 & \mathcal{D}(U) & \cdots & 0 \\ \vdots & \vdots & \ddots & \vdots \\ 0 & 0 & \cdots & \mathcal{D}(U) \end{pmatrix}, \tag{10}$$

with one

$$\mathcal{D}(U) \equiv D \cdot \gamma + m_0 + \mathcal{O}(a^2) \tag{11}$$

for each of the 16 tastes. Thus

$$\det(\Delta \cdot \gamma + m_0)^{1/16} = (\det(\mathcal{D}(U))^{16})^{1/16} \tag{12}$$

$$= |\det(\mathcal{D}(U))| \tag{13}$$

which equals $\det(D \cdot \gamma + m_0)$, up to $a^2$ errors, provided $m_0 > 0$ [17]. The treatment of valence quarks is illustrated in Appendix G.

It is easy to see how the $1/16$ root corrects for taste in particular situations. For example, consider the vacuum polarization of a single pion in a theory of only one massless quark flavor. Still ignoring taste exchange, the dominant infrared contributions come from the quark diagrams shown in Fig. 2 (gluons, to all orders, are implicit in these diagrams). The first diagram, with its double quark loop, has contributions from $16^2$ identical massless pions, corresponding to configurations where the quark and antiquark each carries a momentum close to an integer multiple of $\pi/a$ (and is therefore close to being on shell). This diagram is multiplied by $1/16^2$ since there are two quark loops, thereby giving the contribution of a single massless pion. The second diagram involves quark annihilation into gluons, and has contributions from 16 identical massless pions, corresponding to configurations where the quark and antiquark each carries a momentum close to the same $\zeta\pi/a$ (so they can annihilate into low-momentum gluons). This diagram is multiplied by $1/16$ since there is only one quark loop, thereby giving the contribution again of a single massless pion but now with an insertion from the gluon decay. Inserting additional annihilation kernels results in a geometric series of insertions in the propagator of a single massless pion that shifts the pion's mass away from zero, as expected in a $U(1)$ flavor theory.

Such patterns are disturbed by taste-exchange interactions like that in Fig. 1. For example, these interactions cause mixing between the different tastes of pion in Fig. 2. This mixing lifts the degeneracy in the pion masses so that different tastes of pion are only approximately equivalent. Consequently the "$1/16$-root rule" gives results that correspond only approximately to a single pion.

Our analysis of the 16-taste theory, without taking the $1/16$ root, indicates that taste-exchange errors are $\mathcal{O}(a^2)$, as discussed above, and therefore vanish in the continuum limit. It is not immediately obvious, however, that this is the case when the $1/16$ root is used to reduce the number of tastes to one. Taste exchange generates $\mathcal{O}(a^2)$ off-axis matrix elements in Eq. (10), and one might worry that taking the root could somehow enhance the importance of such terms by canceling the explicit powers of $a^2$ coming from the (dimension-six) taste-exchange operators. The $1/16$-root trick is certainly correct if the off-axis elements are zero; the only question is whether the limit is smooth. The off-axis elements can also lead to such anomalies as unitarity violations with the $1/16$ root, but these will vanish in the continuum if the limit is smooth (since they are not there when the off-axis elements are zero); and short of the continuum limit, they will be suppressed.

Although not proven conclusively, it seems very likely that the continuum limit is smooth, and that taste-exchange effects are suppressed by $a^2$. A wide variety of possible issues is discussed at length in [14]. Here we note just two. First, one might worry that infrared divergences could cancel explicit powers of $a^2$ from the off-axis elements when using the $1/16$ root. Such divergences are cut off by the pion mass, however, and so cannot cancel $a^2$s as $a \rightarrow 0$ provided the continuum limit is taken *before* the chiral limit. Chiral perturbation theory is the appropriate tool for exploring infrared divergences, and explicit calculations, using chiral perturbation theory for several different physical quantities, indicate that all effects from taste exchange are suppressed by $a^2$ [18]. These calculations are supported by detailed simulations at multiple lattice

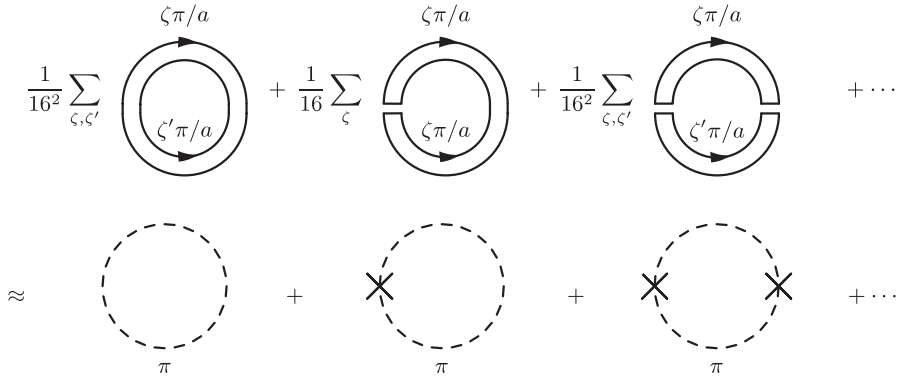


FIG. 2. Infrared contributions from (naive lattice) quark vacuum polarization corresponding to a pion vacuum polarization loop in a simulation of one flavor. The sums are over all infrared sectors, where quarks have momenta near $p_\mu = \zeta_\mu \pi/a$ for one of the 16 $\zeta$s consisting of just 0s and 1s. The factors of $1/16$ are from the $1/16$ rule (Eq. (10)) and cancel the sums. Gluons, to all orders, are implicit in these diagrams.

spacings; for example, the measured splittings between pions of different tastes vanish like $a^2$ (up to powers of $\alpha_s(\pi/a)$) [16].

The infrared spectra of the naive-quark operator $\Delta \cdot \gamma$ and improved versions of it have been studied carefully in simulations at current lattice spacings [19]. These studies show how eigenvalues cluster into increasingly degenerate multiplets of 16 as the lattice spacing vanishes, which is precisely what must happen if the $1/16$-root trick is to work. In particular it is clear from these studies that the topological properties of improved naive quarks are correct provided, again, the continuum limit is taken before the chiral limit—that is, there is a minimum quark mass that can be used for any given lattice spacing if one wants to model quark-instanton interactions accurately, but this minimum mass decreases like $a^2$ as $a \to 0$ [20].

A second issue concerns the possibility that ultraviolet divergences might cancel the explicit $a^2$s from taste-exchange amplitudes, leading to a nonsmooth continuum limit. These divergences can be analyzed perturbatively, however, because of asymptotic freedom. Although formal proofs have yet to be completed, no pathologies are expected from perturbation theory [14], and none have appeared in any of the many detailed perturbative calculations, some through three-loop order, that have been completed for the naive-quark theory and improved versions of it (see, for example, [3]).

These arguments all reenforce our confidence in naive-quark actions (and staggered quarks) and the $1/16$-root trick, and this confidence is greatly enhanced by the many very accurate simulations to date that have been carefully compared with the experiment (for example, [1–5]). Consequently, while taste exchange can lead to anomalies, we expect that these are suppressed in the continuum limit. They are further, and more efficiently, suppressed through Symanzik improvement of the action, which reduces taste-exchange amplitudes even at constant lattice spacing. We now discuss this strategy.

### B. Tree-level Symanzik improvement

The discretization errors in the naive-quark action come from two sources. The more conventional of these corrects the finite-difference approximation to the derivatives in the action: one replaces [6]

$$\Delta_\mu \to \Delta_\mu - \frac{a^2}{6}\Delta_\mu^3 \tag{14}$$

in the naive-quark action (Eq. (1)). The $a^2$ correction is often referred to as the "Naik term."

Less conventional is a correction to remove leading-order taste-exchange interactions [8–10]. As discussed in the previous section, these interactions result from the exchange of single gluons carrying momenta close to $\zeta\pi/a$ for one of the 15 nonzero $\zeta$s ($\zeta_\mu \in \mathbb{Z}_2$). Since these gluons are highly virtual, such interactions are effectively the same as four-quark contact interactions and could be canceled by adding four-quark operators to the quark action. These operators affect physical results in $\mathcal{O}(a^2)$ since they have dimension six. A simpler alternative to four-quark operators is to modify the gluon-quark vertex, $\bar{\psi}\gamma_\mu U_\mu \psi + \cdots$, in the original action by introducing a form factor $f_\mu(q)$ that vanishes for (taste-changing) gluons with momenta $q = \zeta\pi/a$ for each of the 15 nonzero $\zeta$s. In fact the form factor for direction $\mu$ need not vanish when $\zeta_\mu = 1$ since the original interaction already vanishes in that case. Consequently we want a form factor where

$$f_\mu(q) \to \begin{cases} 1 & \text{for } q \to 0 \\ 0 & \text{for } q \to \zeta\pi/a, \text{ where } \zeta^2 \neq 0, \zeta_\mu = 0. \end{cases} \tag{15}$$

We can introduce such a form factor by replacing the link operator $U_\mu(x)$ in the action with $\mathcal{F}_\mu U_\mu(x)$ where smearing operator $\mathcal{F}_\mu$ is defined by

$$\mathcal{F}_\mu \equiv \prod_{\rho\neq\mu}\left(1+\frac{a^2\delta_\rho^{(2)}}{4}\right)\Bigg|_{\text{symm.}} \tag{16}$$

and $\delta_\rho^{(2)}$ approximates a covariant second derivative when acting on link fields:

$$\delta_\rho^{(2)}U_\mu(x) \equiv \frac{1}{a^2}(U_\rho(x)U_\mu(x+a\hat{\rho})U_\rho^\dagger(x+a\hat{\mu}) - 2U_\mu(x) + U_\rho^\dagger(x-a\hat{\rho})U_\mu(x-a\hat{\rho})U_\rho(x-a\hat{\rho}+a\hat{\mu})). \tag{17}$$

This works because $\delta_\rho^{(2)} \approx -4/a^2$ (and $\mathcal{F}_\mu$ vanishes) when acting on a link field that carries momentum $q_\rho \approx \pi/a$. This kind of link smearing is referred to as "Fat7" smearing in [7].

Smearing the links with $\mathcal{F}_\mu$ removes the leading $\mathcal{O}(a^2)$ taste-exchange interactions, but introduces new $\mathcal{O}(a^2)$ errors. These can be removed by replacing $\mathcal{F}_\mu$ with [10]

$$\mathcal{F}_\mu^{\text{ASQTAD}} \equiv \mathcal{F}_\mu - \sum_{\rho\neq\mu}\frac{a^2(\delta_\rho)^2}{4}, \tag{18}$$

where $\delta_\rho$ approximates a covariant first derivative:

$$\delta_\rho U_\mu(x) \equiv \frac{1}{2a}(U_\rho(x)U_\mu(x+a\hat{\rho})U_\rho^\dagger(x+a\hat{\mu}) - U_\rho^\dagger(x-a\hat{\rho})U_\mu(x-a\hat{\rho})U_\rho(x-a\hat{\rho}+a\hat{\mu})). \tag{19}$$

The new term has no effect on taste exchange but (obviously) cancels the $\mathcal{O}(a^2)$ part of $\mathcal{F}_\mu$. Correcting the derivative, as in Eq. (14), and replacing links by $a^2$-accurate smeared links removes all tree-level $\mathcal{O}(a^2)$ errors in the naive-quark action. The result is the widely used ASQTAD action [10],

$$\sum_x \bar{\psi}(x)\left(\sum_\mu \gamma_\mu\left(\Delta_\mu(V) - \frac{a^2}{6}\Delta_\mu^3(U)\right) + m_0\right)\psi(x), \tag{20}$$

where, in the first difference operator,

$$V_\mu(x) \equiv \mathcal{F}_\mu^{\text{ASQTAD}}U_\mu(x). \tag{21}$$

In practice, operator $V_\mu$ is usually tadpole improved [21]; in fact, however, tadpole improvement is not needed when links are smeared and reunitarized [22,23].

### C. *c* quarks

The tree-level discretization errors in the ASQTAD action are $\mathcal{O}((ap_\mu)^4)$, which are negligible ($< 1\%$) for light quarks. When applied to $c$ quarks, however, these errors will be larger. The most important errors in this case are associated with the quark's energy, rather than its 3-momentum, since $c$ quarks are typically nonrelativistic in $\psi$s, $D$s, and other systems of current interest. Consequently $E \approx m \gg \mathbf{p}$ and the largest errors are $\mathcal{O}((am)^4)$ or 6% at current lattice spacings ($am_c \approx 0.5$). Such errors show up, for example, in the tree-level dispersion relation of the quark where:

$$c^2(0) \equiv \lim_{\mathbf{p}\to 0}\frac{E^2(\mathbf{p}) - m^2}{\mathbf{p}^2} = 1 + \frac{9}{20}(am)^4 + \frac{1}{7}(am)^6 + \cdots. \tag{22}$$

This dominant (tree-level) error can be removed by retuning the coefficient of the $a^2\gamma_\mu\Delta_\mu^3$ (Naik) term in the action:

$$\sum_x \bar{\psi}(x)\left(\sum_\mu \gamma_\mu\left(\Delta_\mu - \frac{a^2}{6}(1+\epsilon)\Delta_\mu^3\right) + m_0\right)\psi(x), \tag{23}$$

where parameter $\epsilon$ has expansion

$$\epsilon = -\frac{27}{40}(am)^2 + \frac{327}{1120}(am)^4 - \frac{5843}{53\,760}(am)^6 + \frac{153\,607}{3\,942\,400}(am)^8 - \cdots. \tag{24}$$

With this choice of $\epsilon$ and keeping just the terms shown, $c^2 = 1 + \mathcal{O}((am)^{12})$. Only the first term in $\epsilon$'s expansion is essential for removing $(am)^4$ errors; the remaining terms remove errors to higher orders in $am$ but leading order in $v/c$, the quark's typical velocity. In practice, terms beyond the first few are negligible though trivial to include.

Note that the bare mass $m_0$ in the quark action is related to the tree-level quark mass and wave function renormalization $Z_2$ by

$$m_0 = mZ_2 \tag{25}$$

$$= m\left(1 + \frac{3}{80}(am)^4 - \frac{23}{2240}(am)^6 + \cdots\right) \tag{26}$$

for this choice of $\epsilon$. This formula is useful for extracting the corrected bare quark mass, $m$, from a tuned value of $m_0$.

To examine the tree-level errors in this modified ASQTAD action, it is useful to make a nonrelativistic expansion since, as we indicated, heavy quarks are generally nonrelativistic in the systems of interest. This expansion is easy because the action is identical in form to the continuum Dirac equation, and consequently has the same nonrelativistic expansion but with

$$D_\mu \to \Delta_\mu - \frac{a^2}{6}(1+\epsilon)\Delta_\mu^3. \tag{27}$$

At tree level,

$$\Delta_\mu \to \sinh(aD_t - am)/a, \tag{28}$$

when we replace

$$\psi \to \exp(-mt)\psi, \tag{29}$$

where $m$ is the quark mass. This redefinition removes the

rest mass from all energies. Expanding in powers of $1/m$, we then obtain the tree-level nonrelativistic expansion of the modified ASQTAD action:

$$\sum \psi^\dagger_{\rm NR}\Big(D_t - \frac{\mathbf{D}^2}{2m} - c_K\frac{\mathbf{D}^4}{8m^3} - \frac{g\sigma\cdot\mathbf{B}}{2m} + c_E\frac{ig[\mathbf{D}\cdot,\mathbf{E}]}{8m^2} - c_E\frac{g\sigma\cdot(\mathbf{D}\times\mathbf{E}-\mathbf{E}\times\mathbf{D})}{8m^2} + \cdots\Big)\psi_{\rm NR}, \quad (30)$$

where

$$c_K = 1 - \tfrac{9}{10}(am)^4 + \tfrac{29}{280}(am)^6 - \cdots, \quad (31)$$

$$c_E = 1 - \tfrac{3}{80}(am)^4 + \tfrac{23}{2240}(am)^6 - \cdots. \quad (32)$$

The coefficients of all terms through order $1/m$ have no $am$ errors at tree level. In particular the $\sigma\cdot\mathbf{B}$ term is correct at tree level once $m$ is tuned (nonperturbatively). The coefficients of the remaining terms shown are off by less than 6% and 1% for charm quarks on current lattices ($am \approx 1/2$), which should lead to errors of order $(am)^4(v/c)^2 \approx 2\%$ or less in charmonium analyses and less than 0.5% for $D$ physics. (Errors should actually be considerably smaller than this because of dimensionless factors like the 1/8 in the $\mathbf{D}^4$ term.) Other tree-level errors, which are order $(a\mathbf{p})^4$ and $\epsilon(a\mathbf{p})^2/6$, should also be less than 1% for $a \approx 0.1$ fm.

## III. SYMANZIK IMPROVEMENT AT ONE-LOOP ORDER

One-loop errors, which are $\mathcal{O}(\alpha_s(ap)^2)$, should be no more than a percent or so for light quarks and current lattice spacings. Taste-changing errors, however, have generally been much larger than expected. These errors also bear directly on the validity of the 1/16-root trick for accounting for taste in the vacuum polarization. For this reason it is worth trying to further suppress taste-exchange errors beyond what has been accomplished at tree level. We show how to do this in this section.

The only other one-loop effects that are important at the level of a few percent are $\alpha_s(am)^2$ for heavy quarks, and, in particular, the charm quark. We show how to correct for these errors in the Sec. III B.

### A. Light quarks

One-loop taste exchange comes only from the diagrams shown in Fig. 3; other one-loop diagrams vanish because of the tree-level improvements. Again the gluons in these diagrams transfer momenta of order $\zeta\pi/a$, and so are highly virtual. Consequently, the correction terms in the corrected action that cancel these will involve current-current interactions that conserve overall taste (because of momentum conservation). There are 28 such terms in the massless limit for the staggered-quark action (see Appendix F):

$$\begin{aligned}2\Delta\mathcal{L}_{\rm contact} = {} & d_5^{(5\mu)}|\mathcal{J}_5^{(5\mu)}|^2 + d_{5\mu\nu}^{(5\nu)}|\mathcal{J}_{5\mu\nu}^{(5\nu)}|^2 + d_\nu^{(\mu\nu)}|\mathcal{J}_\nu^{(\mu\nu)}|^2 + d_{5\nu}^{(5\mu\nu)}|\mathcal{J}_{5\nu}^{(5\mu\nu)}|^2 + d_{\mu\nu}^{(\nu)}|\mathcal{J}_{\mu\nu}^{(\nu)}|^2 + d_1^{(\mu)}|\mathcal{J}_1^{(\mu)}|^2 + d_{5\mu}^{(5)}|\mathcal{J}_{5\mu}^{(5)}|^2 \\ & + d_1^{(5\mu)}|\mathcal{J}_1^{(5\mu)}|^2 + d_{\mu\nu}^{(5\nu)}|\mathcal{J}_{\mu\nu}^{(5\nu)}|^2 + d_\nu^{(5\mu\nu)}|\mathcal{J}_\nu^{(5\mu\nu)}|^2 + d_{5\nu}^{(\mu\nu)}|\mathcal{J}_{5\nu}^{(\mu\nu)}|^2 + d_{5\mu\nu}^{(\nu)}|\mathcal{J}_{5\mu\nu}^{(\nu)}|^2 + d_5^{(\mu)}|\mathcal{J}_5^{(\mu)}|^2 \\ & + d_\mu^{(5)}|\mathcal{J}_\mu^{(5)}|^2 + (\text{color octet } \mathcal{J}\text{s with } d_n^{(t)} \to \tilde{d}_n^{(t)}),\end{aligned} \quad (33)$$

where sums over indices are implicit and $\nu \neq \mu$. The currents $\mathcal{J}_n^{(s)}$ in the first 14 operators are color-singlets with taste $s$ and spinor structure $n$, while the last 14 operators are the same but with color octet currents. The precise definitions of these currents are given in Appendix E.

We have computed the coupling constants $d_n^{(s)}$ and $\tilde{d}_n^{(s)}$ for the tree-level improved theory; the results are presented in Table II (see also Appendix F). Armed with these one could incorporate $\Delta\mathcal{L}_{\rm contact}$ into simulations, removing all one-loop taste exchange. This procedure is complicated to implement, however. A simpler procedure is suggested by the results in [11]. That analysis shows that repeated smearing of the links further reduces the mass splittings between pions of different taste.

This result is not surprising given the perturbative origins of taste exchange. The dominant taste-exchange interactions (in ASQTAD) come from the one-loop diagrams in Fig. 3. The largest contributions to these diagrams come from large loop momenta, $k = \mathcal{O}(\zeta\pi/2a)$. Smearing the links introduces form factors that suppress high momenta, leaving low momenta unchanged, and therefore should suppress this sort of one-loop correction. The links in the ASQTAD action are smeared, but the operator $\mathcal{F}_\mu^{\rm ASQTAD}$, which smears links in the $\mu$ direction, introduces additional links in orthogonal directions (to preserve gauge invariance) that are not smeared. Smearing the links multiple times guarantees that all links are smeared, and high momenta are suppressed.

There are three problems associated with multiple smearing. One is that it introduces new $\mathcal{O}(a^2)$ discretization errors, and these errors grow with additional smearing. The action presented in [11] suffers from this problem. The $a^2$ errors can be avoided by using an $a^2$-improved smearing operator, such as $\mathcal{F}_\mu^{\rm ASQTAD}$ (Eq. (18)). Replacing smearing operator

$$\mathcal{F}_\mu^{\rm ASQTAD} \to \mathcal{F}_\mu^{\rm ASQTAD}\mathcal{F}_\mu^{\rm ASQTAD} \quad (34)$$

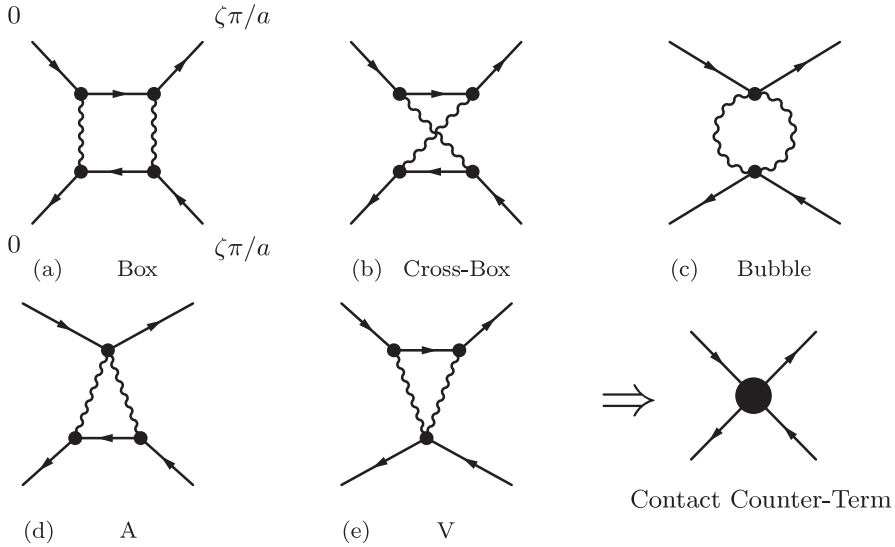


FIG. 3. The only one-loop diagrams that result in $q\bar{q} \to q\bar{q}$ taste exchange for ASQTAD quarks. Diagrams with additional external quark lines are suppressed by additional powers of $a^2$.

TABLE II. $\mathcal{O}(\alpha_s)$ coefficients for the couplings in $\mathcal{L}_{\text{contact}}$ (Eq. (33)) for three different light-quark actions and massless quarks. Terms not listed have zero coefficients in this order. Results are given for the unimproved (Wilson) gluon action, and, in the ASQTAD case, also for the standard Lüscher-Weisz action. Results for the average coefficient are also given.

| | Unimproved gluons | | | Improved gluons |
|---|---|---|---|---|
| | ASQTAD | HISQ | HYP | ASQTAD |
| Octet: | | | | |
| $\tilde{d}_5^{(5\mu)}$ | 1.41 | 0.19 | 0.02 | 0.77 |
| $\tilde{d}_{5\mu\nu}^{(5\nu)}$ | 0.46 | 0.00 | 0.08 | 0.25 |
| $\tilde{d}_1^{(5\mu)}$ | 0.23 | 0.01 | 0.00 | 0.16 |
| $\tilde{d}_{\mu\nu}^{(5\nu)}$ | 0.38 | 0.02 | 0.01 | 0.27 |
| $\tilde{d}_\nu^{(\mu\nu)}$ | 0.34 | 0.08 | 0.04 | 0.19 |
| $\tilde{d}_{5\nu}^{(5\mu\nu)}$ | 0.35 | 0.03 | 0.02 | 0.19 |
| $\tilde{d}_\nu^{(5\mu\nu)}$ | 0.08 | 0.00 | 0.01 | 0.05 |
| $\tilde{d}_{5\nu}^{(\mu\nu)}$ | 0.20 | 0.00 | 0.01 | 0.13 |
| $\tilde{d}_{\mu\nu}^{(\nu)}$ | 0.20 | 0.01 | 0.02 | 0.11 |
| $\tilde{d}_1^{(\mu)}$ | 0.31 | 0.01 | 0.01 | 0.17 |
| $\tilde{d}_{5\mu\nu}^{(\nu)}$ | 0.06 | 0.00 | 0.00 | 0.04 |
| $\tilde{d}_5^{(\mu)}$ | 0.07 | 0.00 | 0.01 | 0.04 |
| $\tilde{d}_{5\mu}^{(5)}$ | 0.17 | 0.00 | 0.01 | 0.09 |
| $\tilde{d}_\mu^{(5)}$ | 0.06 | 0.00 | 0.00 | 0.04 |
| Singlet: | | | | |
| $d_5^{(5\mu)}$ | 0.76 | 0.10 | 0.01 | 0.41 |
| $d_1^{(5\mu)}$ | 0.12 | 0.00 | 0.00 | 0.09 |
| $d_\nu^{(\mu\nu)}$ | 0.18 | 0.05 | 0.02 | 0.10 |
| $d_\nu^{(5\mu\nu)}$ | 0.04 | 0.00 | 0.00 | 0.03 |
| $d_{\mu\nu}^{(\nu)}$ | 0.11 | 0.01 | 0.01 | 0.06 |
| $d_{5\mu\nu}^{(\nu)}$ | 0.03 | 0.00 | 0.00 | 0.02 |
| $d_{5\mu}^{(5)}$ | 0.09 | 0.00 | 0.00 | 0.05 |
| Avg. $d$, $\tilde{d}$ | 0.23 | 0.02 | 0.02 | 0.13 |

in the quark action, for example, smears all links but does not introduce new tree-level $a^2$ errors.

The second problem with multiple smearings is that they replace a single link in the naive action by a sum of a very large number of products of links. This explosion in the number of terms does not affect single-gluon vertices on quark lines, by design, but leads to a $\sqrt{N}$-growth in the size of two-gluon vertices where $N$ is the number of terms in the sum. The $\sqrt{N}$-growth enhances one-loop diagrams with two-gluon vertices, canceling much of the benefit obtained from smearing. This problem is remedied by reunitarizing the smeared link operator: that is we replace

$$\mathcal{F}_\mu^{\text{ASQTAD}} \to \mathcal{F}_\mu^{\text{ASQTAD}} \mathcal{U} \mathcal{F}_\mu^{\text{ASQTAD}}, \tag{35}$$

where operator $\mathcal{U}$ unitarizes whatever it acts on. A smeared link that has been unitarized is bounded (by unity) and so cannot suffer from the $\sqrt{N}$ problem. Although we verified that it is unnecessary to make the unitarized link into an $SU(3)$ matrix—simple unitarization is adequate—the results given in this paper use links that are projected back onto $SU(3)$. Reunitarizing has no effect on the single-gluon vertex, and therefore does not introduce new $\mathcal{O}(a^2)$ errors.

The doubly smeared operator is simplified if we rearrange it as follows

$$\mathcal{F}_\mu^{\text{HISQ}} \equiv \left(\mathcal{F}_\mu - \sum_{\rho \neq \mu} \frac{a^2 (\delta_\rho)^2}{2}\right) \mathcal{U} \mathcal{F}_\mu, \tag{36}$$

where the entire correction for $a^2$ errors is moved to the outermost smearing. Our new "HISQ" discretization of the quark action is therefore

$$\sum_x \bar{\psi}(x)(\gamma \cdot \mathcal{D}^{\text{HISQ}} + m)\psi(x), \tag{37}$$

where

$$\mathcal{D}_\mu^{\mathrm{HISQ}} \equiv \Delta_\mu(W) - \frac{a^2}{6}(1+\epsilon)\Delta_\mu^3(X) \tag{38}$$

and now, in the first difference operator,

$$W_\mu(x) \equiv \mathcal{F}_\mu^{\mathrm{HISQ}} U_\mu(x), \tag{39}$$

while in the second,

$$X_\mu(x) \equiv \mathcal{U}\mathcal{F}_\mu U_\mu(x). \tag{40}$$

The third problem with smearing is that previous work has only demonstrated its impact on the mass splittings between pions with different tastes. For small masses, there are only five degenerate multiplets of pion. Consequently showing that smearing reduces the splittings between the pion multiplets does not guarantee that all 28 taste-exchange terms in the quark action (Eq. (33)) are suppressed; and, therefore, it does not guarantee that taste-exchange effects are generally suppressed (other than in the pion mass splittings).

To examine this issue, we recomputed the one-loop coefficients for all of the leading taste-exchange correction terms in the action (Eq. (33)) using the HISQ action, as well as the HYP action from [11]. These coefficients provide a direct measure of the residual one-loop taste-exchange errors in each theory. The results are derived in Appendix F and presented in Table II. The HISQ coefficients are on average an order of magnitude smaller than the ASQTAD coefficients. Thus the HISQ action (Eqs. (37)–(40)) has negligible one-loop taste-exchange corrections, and the complicated contact terms of Eq. (33) are not needed. In Sec. IV A we demonstrate that this perturbative improvement leads to significantly improved nonperturbative results, now that two-loop and higher-order taste exchange, together with higher-dimension contributions, are all that is left. The HYP action gives coefficients similar in size to HISQ.

### B. *c* quarks

Many new taste-preserving operators would need to be added to the HISQ action in order to remove all order $\alpha_s a^2$ errors. The leading operators are listed in Table III. None of these is relevant at the few-percent level for light quarks, but terms that enter in relative order $\alpha_s(am_c)^2$ might change answers by as much as 5%–10% for $c$ quarks on current lattices, where $am_c \approx 0.5$ and $\alpha_s \approx 1/3$. High-precision work requires that these errors be removed.

Nonrelativistic expansions of the various operators in Table III show that only the first, the Naik term, can cause errors in order $\alpha_s(am_c)^2$. All of the others result in harmless renormalizations or are suppressed by additional powers of $v/c$, and so contribute only at the level of 2%–3% or less for $\psi$s and less than 1% for $D$s. We can remove all $\alpha_s(am_c)^2$ errors by including radiative corrections in the $\epsilon$ parameter that multiply the Naik term (Eq. (23)).

TABLE III. Relative errors associated with the leading (for charm quarks) taste-preserving operators that enter the HISQ action in one-loop order. Note that $\alpha_s \approx 1/3$, $(am)^2 \approx 1/4$, and $(v/c)^2 \approx 1/3$ for $\psi$s (1/10 for $D$s) for lattice spacings of order 0.1 fm. The errors listed are relative to the binding energy which is of order 500 MeV for both $\psi$s and $D$s. Some of the operators are related to others in the same grouping by the equations of motion, and so are redundant.

| Operator $a^2\bar{\psi}D_\mu^3\gamma_\mu\psi$ | $\psi$ physics $\alpha_s(am)^2$ | $D$ physics $\alpha_s(am)^2$ |
|---|---|---|
| $a^2 m\bar{\psi}\sigma\cdot gF\psi$<br>$a^2\bar{\psi}D^2 D\cdot\gamma\psi$<br>$a^2\bar{\psi}(D\cdot\gamma)^3\psi$<br>$a^2 m\bar{\psi}D^2\psi$<br>$a^2\bar{\psi}\sigma\cdot gFD\cdot\gamma\psi$ | $\alpha_s(v/c)^2(am)^2$ | $\alpha_s(v/c)(am)^2$ |
| $a^2\bar{\psi}D\cdot gF\cdot\gamma\psi$<br>$a^2(\bar{\psi}\gamma\psi)^2$<br>$a^2(\bar{\psi}\gamma\gamma_5\psi)^2$ | $\alpha_s(v/c)^2(am)^2$ | $\alpha_s(v/c)^2(am)^2$ |

There are two ways to compute the radiative correction to $\epsilon$. One is nonperturbative: $\epsilon$ is adjusted until the relativistic dispersion relation,

$$c^2(\mathbf{p}) \equiv \frac{E^2(\mathbf{p}) - m^2}{\mathbf{p}^2} = 1, \tag{41}$$

computed in a meson simulation is valid for all low three-momenta $\mathbf{p}$.

A simpler procedure is to compute the one-loop correction to $\epsilon$ using perturbation theory—by requiring, for example, the correct dispersion relation for a quark in one-loop order. The result would have the form

$$\epsilon = \epsilon_1\alpha_s - \tfrac{27}{40}(am)^2 + \mathcal{O}(\alpha_s^2, (am)^4), \tag{42}$$

where $\epsilon_1$ depends upon $(am)^2$. As we will show, $\epsilon_1$ turns out to be negligibly small for the HISQ action (but not for ASQTAD).

## IV. APPLICATIONS: LIGHT QUARKS

### A. Pion taste splittings

We tested our perturbative analysis of the suppression of taste exchange by computing the mass splittings between pions of different taste for ASQTAD, HISQ, and a few other variations [24]. For each of these we also computed the one-loop coefficients of the taste-exchange interactions (Eq. (33)) in perturbation theory. We plot the pion mass splittings versus the average size of the perturbative coefficients in Fig. 4. As expected, large coefficients correlate with large mass splittings (and, therefore, large taste-exchange errors). One-loop contributions should dominate when the coefficients are large, and the mass splittings should be roughly proportional to the average coefficient.

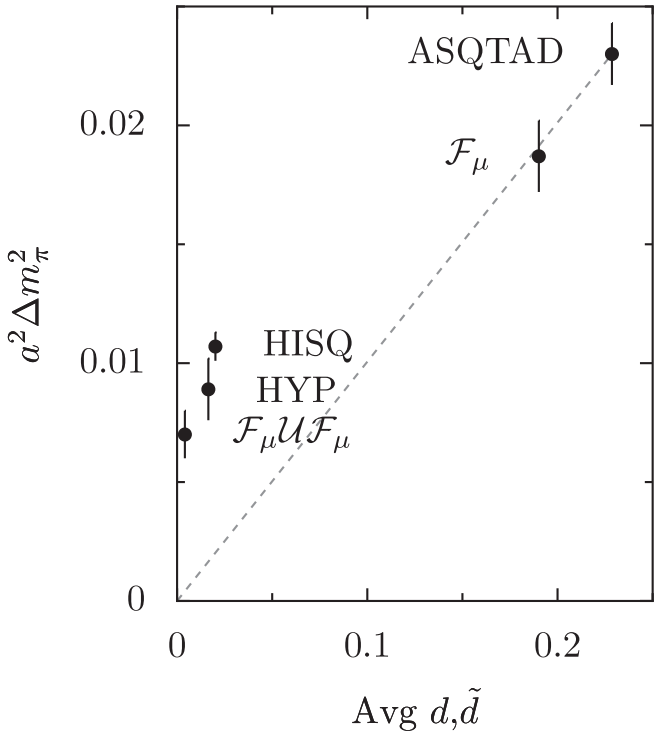


FIG. 4. The splitting between the 3-link and Goldstone (0-link) pions plotted versus the average value of the coefficients of the taste-exchange operators (Eq. (33)) from one-loop perturbation theory. Results are shown for several different smearings of the link field, including those used in ASQTAD (Eq. (18)) and HISQ (Eq. (36)). The pion masses are from simulations with uncorrected gluons at $a \approx 1/10$ fm and no sea quarks.

As the one-loop coefficients become very small, other taste-exchange mechanisms will dominate—higher-dimension operators, higher-order perturbation theory—and splittings will be larger than would be expected from just the one-loop coefficients. Our simulation data is consistent with this pattern.

The pion simulations used in this analysis used uncorrected gluons and omitted quark vacuum polarization. We have repeated our calculation for ASQTAD and HISQ valence quarks in full QCD simulations with $n_f = 3$ light-quark (ASQTAD) vacuum polarization. We find that the pseudoscalar splittings are 3.6(5) times smaller with HISQ than with ASQTAD on lattices with $a = 1/8$ fm, when both valence quarks are $s$ quarks. The splittings are 3.1(7) times smaller on our $1/11$ fm lattices.

The perturbative origins of taste exchange were already evident from the threefold reduction observed in pion splittings when uncorrected staggered quarks were replaced by ASQTAD quarks, which incorporate perturbative corrections that remove taste exchange in tree-level order. Our new results show a similar reduction when one-loop corrections are effectively removed, providing further nonperturbative evidence that taste exchange is perturbative and therefore amenable to Symanzik improvement. Our results confirm our expectation that taste-exchange errors from HISQ are smaller by at least a factor of order $\alpha_s \approx 1/3$ than those from ASQTAD. Consequently the HISQ action will be more accurate than other current competitors because it has negligible one-loop taste exchange and no tree-level $\mathcal{O}(a^2)$ errors.

### B. Bounding taste-exchange errors

The main difference between the ASQTAD and HISQ actions is that taste-exchange effects in the latter should be 3–4 times smaller at the same lattice spacing. Consequently the taste-exchange error in an ASQTAD measurement of some quantity should be bounded approximately by the difference between ASQTAD and HISQ results for that quantity (measured at the same lattice spacing). The bound on taste-exchange errors in the HISQ measurement would then be 3–4 times smaller. The ASQTAD-HISQ difference for any quantity provides a very efficient indicator for the size and importance of taste-exchange errors.

This procedure only provides a bound, not an estimate, because HISQ and ASQTAD also differ in their radiative corrections to currents and coupling constants. Thus an observed ASQTAD-HISQ difference in some quantity could be dominated by differences in uncalculated radiative corrections if the taste-exchange effects are much smaller.

To illustrate how such comparisons are done, we have computed the mass of the $\phi$ meson and the pseudovector decay constant $f_{\eta_s}$ of the $\eta_s$ meson using ASQTAD and HISQ valence quarks for each of our two lattice spacings.

The $\phi$ is unstable and so its mass in a simulation is unusually sensitive to the sea-quark masses and the volume of the lattice (it is *not* "gold-plated" in the sense of [1]). We have not corrected for this sensitivity, but have simulated using fixed physical sea-quark masses and lattice volume. Consequently results for the $\phi$ mass should extrapolate to the same value as $a \to 0$, but this value may be a few tens of MeV larger than the physical mass. The $\eta_s$ is an easy-to-analyze substitute for a $\pi$; it is a $0^{-+}$ $s\bar{s}$ meson, but without valence-quark annihilation (and therefore hypothetical). We tuned the $s$ mass so that the $\eta_s$ masses in each case were all identical (696 MeV) to within $\pm 1$ MeV (statistical/fitting errors only). We evaluated the $\eta_s$ decay constant by computing the matrix element of the pseudoscalar density and multiplying by the bare quark mass (see [2], for example).

Our results, shown in Table IV, suggest significant taste-exchange errors for ASQTAD, particularly in the $1/8$ fm simulation. Looking first at the decay constant, $f_{\eta_s}$, ASQTAD and HISQ differ by 4.6(6)% (see the last column of Table IV). Assuming ASQTAD taste-exchange errors are 3–4 times larger, this difference implies that taste-exchange errors could be 5%–6% in the ASQTAD measurement of this quantity, while only 1%–2% for HISQ.

TABLE IV. Simulation results for decay constant $f_{\eta_s}$ and $\phi$ mass using either ASQTAD or HISQ for the valence quarks from full QCD simulations (with $n_f = 3$ ASQTAD quarks). The first uncertainty quoted is statistical. The second, where quoted, is an overall systematic error associated with setting the lattice spacing scale (from $r_1$); it cancels in ratios. ASQTAD/HISQ ratios at the same lattice spacing have still smaller statistical errors because of strong correlations.

| | $a$ (fm) | ASQTAD | HISQ | ASQTAD/HISQ |
|---|---|---|---|---|
| $f_{\eta_s}$ (MeV): | | | | |
| | 1/8 | 196(3)(3) | 187(3)(3) | 1.046(6) |
| | 1/11 | 185(2)(3) | 182(2)(3) | 1.019(4) |
| $m_\phi$ (GeV): | | | | |
| | 1/8 | 1.119(14)(18) | 1.076(14)(16) | 1.040(9) |
| | 1/11 | 1.057(10)(16) | 1.052(7)(16) | 1.005(6) |

The errors should be half that size or smaller in the $a = 1/11$ fm simulation since these errors vanish like $a^2$ or faster as $a \to 0$. This is consistent with what we observe in our simulations.

The lattice spacing dependence of the separate quantities, as opposed to the ASQTAD/HISQ ratio, is consistent with this picture although statistically much less compelling. The ASQTAD result for $f_{\eta_s}$ on the coarse lattice is 5.9(1.8)% larger than the ASQTAD result on the fine lattice, which is approximately what was suggested by the ASQTAD-HISQ difference. The variation for HISQ, on the other hand, is too small to measure given our statistical errors. Results from both formalisms are consistent with an extrapolated value of 180(4) MeV.

Results for the $\phi$ mass are very similar. These give a final mass of 1.05(2) GeV, which is 30(20) MeV above the mass 1.019 GeV from experiment (and consistent with expectations, as discussed above). These analyses taken together indicate that HISQ is delivering 1%–2% precision already on the coarse lattice, while a significantly smaller lattice spacing (and much more costly simulation) is needed to achieve similar precision from ASQTAD. HISQ taste-exchange errors should be less than 1% on the 1/11 fm lattice for light quarks.

Our tests are only partial because ASQTAD quarks were used for the vacuum polarization in both the HISQ and ASQTAD analyses, but the effects of changes in the vacuum polarization are typically 3–5 times smaller than the effects caused by the same changes in the valence quarks [25]. The agreement between our HISQ results from different lattice spacings indicates that finite-$a$ errors from the vacuum polarization are not large for these lattice spacings.

In past work, taste-exchange errors have been estimated by comparing results from different lattice spacings, relying upon the fact that these errors vanish as $a \to 0$. This example illustrates how the same errors can be reliably bounded by comparing ASQTAD with HISQ results from simulations using only a single lattice spacing. This approach to estimating taste-exchange errors is very efficient. It is almost certainly the simplest way to quantify uncertainties about taste exchange and the validity of the 1/16-root trick for vacuum polarization.

## V. APPLICATIONS: $c$ QUARKS AND CHARMONIUM

As argued in Secs. II C and III B, we expect the ASQTAD action and, especially, the HISQ action to work well for $c$ quarks even though $am_c$ is typically of order 0.4 or larger on current lattices. To achieve high precision (few percent or better), we must tune the Naik term's renormalization parameter $\epsilon$ (Eq. (23)). Here we do this nonperturbatively by computing the speed of light squared, $c^2(\mathbf{p})$ (Eq. (22)), for the $\eta_c$ in simulations with various values of $\epsilon$ and tuning $\epsilon$ until $c^2 = 1$. Our results are summarized in Table V.

The ASQTAD results on the fine lattices show only small errors in $c^2$ even with $\epsilon = 0$. Values for different $\epsilon$s are plotted in Fig. 5, together with an interpolating curve. These data indicate that the optimal choice is $\epsilon = 0.19(5)$ for this lattice spacing and mass. The tree-level prediction for $\epsilon$, from Eq. (24), is $-0.10$, which indicates that radiative corrections in $\epsilon$ are of order $1 \times \alpha_s \approx 0.3$, as expected.

The HISQ results show even smaller $c^2$ errors on the fine lattices. Tuning to $\epsilon = -0.1155$, the tree-level value given by Eq. (24) for $am_c = 0.43$, removes all errors in $c^2$ at the

TABLE V. The speed of light squared, $c^2(\mathbf{p})$, computed from the $\eta_c$'s dispersion relation in simulations using different quark actions. Results are given for different values of the Naik term's renormalization parameter $\epsilon$ (Eq. (23)), the lattice spacings $a$, and the meson's three-momenta $\mathbf{p}$ (in units of the smallest momentum on the lattice which was roughly 0.5 GeV in each case).

| | $\epsilon$ | $am$ | $(\mathbf{p}/p_{\min})^2$ | $c^2(\mathbf{p})$ |
|---|---|---|---|---|
| ASQTAD (1/11 fm): | 0 | 0.38 | 2 | 0.962(9) |
| | 0.3 | 0.38 | 2 | 1.020(11) |
| | 0.4 | 0.38 | 2 | 1.036(11) |
| HISQ (1/11 fm): | 0 | 0.43 | 2 | 1.029(11) |
| | −0.115 | 0.43 | 1 | 0.985(16) |
| | −0.115 | 0.43 | 2 | 0.992(13) |
| | −0.115 | 0.43 | 3 | 1.014(15) |
| | −0.115 | 0.43 | 4 | 0.991(11) |
| HISQ (1/8 fm): | 0 | 0.67 | 1 | 1.190(20) |
| | −1 | 0.67 | 1 | 0.560(10) |
| | −0.35 | 0.67 | 1 | 0.904(15) |
| | −0.28 | 0.67 | 1 | 0.950(15) |
| | −0.21 | 0.66 | 1 | 1.008(13) |
| | −0.21 | 0.66 | 2 | 1.017(10) |
| | −0.21 | 0.66 | 3 | 1.019(12) |
| | −0.21 | 0.66 | 4 | 1.007(7) |

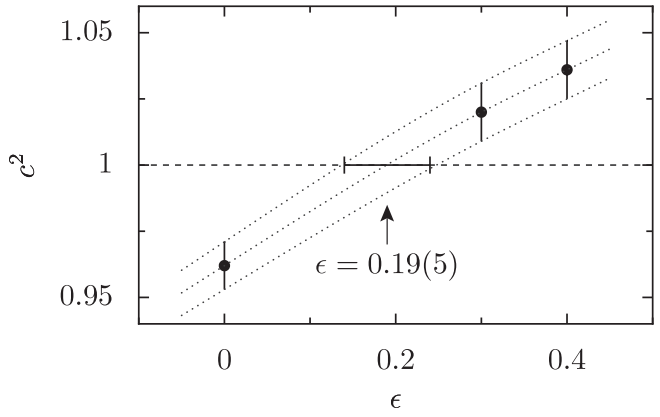


FIG. 5. The speed of light squared, $c^2(\mathbf{p})$, computed for an $\eta_c$ meson using the ASQTAD action with $\mathbf{p} = (p_{\min}, p_{\min}, 0)$ and different Naik-term renormalizations $\epsilon$, where $p_{\min}$ is the smallest lattice momentum possible (approximately 500 MeV here). The correct value, $\epsilon = 0.19(5)$, occurs at the intersection of the interpolating line with the line $c^2 = 1$, as shown. Here $am_c = .38$.

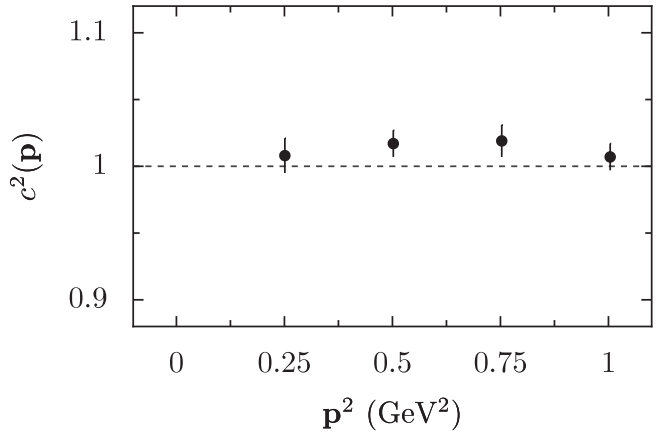


FIG. 6. The speed of light squared, $c^2(\mathbf{p}^2)$, for $\eta_c$ mesons at different momenta on a lattice where $am_c \approx 0.66$ for the HISQ action with $\epsilon = -0.21$. A comparison with other results from Table V suggests that choosing $\epsilon = -0.22$ would move all points down onto the line $c^2 = 1$ to within errors.

level of 1%. This suggests that one-loop and higher-order radiative corrections in $\epsilon$ are negligible for HISQ compared with the tree-level corrections. The dominance of tree-level contributions is confirmed by our HISQ analysis using the coarser lattice spacing, where $am_c \approx 0.66$. Here, we found the optimal value $\epsilon = -0.22(3)$ again by tuning $\epsilon$ until $c^2 = 1$ for a low-momentum $\eta_c$. (We overshot slightly and did simulations for $\epsilon = -0.21$ rather than $-0.22$.) Our tuned $\epsilon$ compares quite well with the tree-level prediction of $-0.246$ from Eq. (24). Consequently it is quite likely that the tree-level formula is sufficiently accurate for most practical applications today.

Note that setting $\epsilon = -1$ cancels out the Naik term completely. Tree-level errors are then order $a^2$ rather than order $a^4$, as in the HISQ action. Table V shows that these $a^2$ errors cause $c^2$ to be off by almost a factor of 2. This example underscores the importance of using $a^2$-improved actions in high-precision work.

On the coarse lattice, we use the $c^2(\mathbf{p})$ with $p = p_{\min}$, the smallest nonzero momentum on our lattice, to tune $\epsilon$. It is important to verify that the tuned action gives the correct dispersion relation for other momenta as well. The data in Fig. 6 demonstrate that errors are less than a couple percent for meson momenta out to 1 GeV even on the coarse lattice where $am_c = 0.66$. Indeed, the errors would probably have been smaller ($< 1\%$) had we tuned $\epsilon$ a little more accurately.

We examined the spectrum of the $\psi$ meson family to further test the precision of our formalism. We used the $1/11$ fm lattices where $am_c \approx 0.4$, and therefore we expect errors of order 1%–2% of the binding energy, or 5–10 MeV (see Sec. III B). A particularly sensitive test is the hyperfine mass splitting between the $\psi$ and $\eta_c$. We tuned the bare $c$ mass until the mass of the local (and lightest) $\eta_c$ in our simulation agreed with the experiment. Since there are no other free parameters in our action, the simulation then predicts a mass for the $\psi$. As is clear from Fig. 7, the $\psi$ mass in the simulation is quite accurate—certainly within the 5–10 MeV we expected.

The data shown in this last figure also bound taste-exchange errors. As shown there, different tastes of the $\eta_c$ have different masses, because of taste-exchange interactions. The maximum spread in the masses for the HISQ action, however, is only 9 MeV. This is much smaller than the spread from the ASQTAD action, where the splitting between, for example, the 0-link and 1-temporal-link $\eta_c$ masses is 40 MeV (compared to only 3 MeV for the same

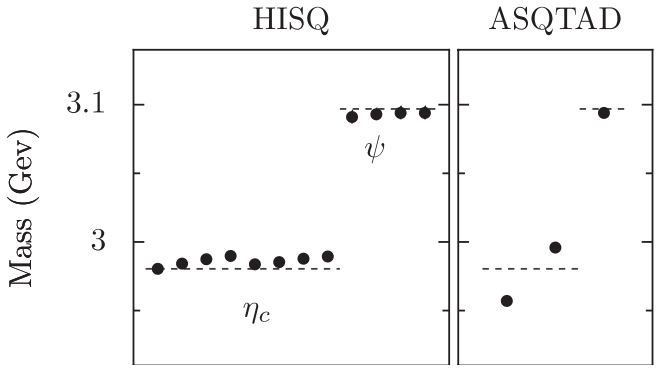


FIG. 7. Masses for different tastes of the $\eta_c$ and $\psi$ using HISQ and ASQTAD $c$ quarks with $\epsilon = 0$ on a $1/11$ fm lattice ($am_c \approx 0.4$). For HISQ, $\eta_c$s are given (from left to right) for the 0, 1, 2, and 3 spatial link tastes, without and then with a temporal link; only the spatial splittings are given for the $\psi$. For ASQTAD, $\eta_c$ results are given for only the 0-link and 1-temporal-link operators, and $\psi$ results for only the 0-link operator. The dashed lines indicate the results from the experiment. Error bars are of order the size of the plot symbols.

splitting with HISQ). (Uncorrected staggered quarks also show very large splittings [26].) Note also that the spread in the $\psi$s is 3 times smaller than the spread in the $\eta_c$s. This is typical; the masses of mesons other than pseudoscalars are much less sensitive to taste-exchange effects.

The $\psi - \eta_c$ hyperfine splitting, for 0-link mesons in each case, is 109(3) MeV in our $1/11$ fm simulation with tuned $\epsilon$ ( $= -0.115$). The 3% uncertainty is almost entirely due to tuning uncertainties in the lattice spacings since these uncertainties enter twice: once for converting the splitting from lattice to physical units, and once through uncertainties in the $c$ mass, which are themselves controlled by uncertainties in $a^{-1}$ [12]. Our HISQ result is somewhat smaller than the current experimental result of 117(1) MeV [27], but it needs three further corrections. (It is also worth noting that the current Particle Data Group average of 117 MeV is somewhat larger than the most recent experiments which find values in the range 113–115 MeV with uncertainties of 1–2 MeV; see [27].)

The first correction comes from the operators in Table III that must be added to the HISQ Lagrangian in order to remove further discretization errors. Of these the most important for the hyperfine splitting is

$$\delta\mathcal{L}_{\rm hfs} = c_{\rm hfs} a^2 m_c \bar{\psi}\sigma \cdot F\psi, \tag{43}$$

where $c_{\rm hfs} = \mathcal{O}(\alpha_s)$. This will affect the hyperfine splitting in relative order $\alpha_s(am_c)^2$, or at the level of $\pm 5$ MeV. The coefficient $c_{\rm hfs}$ is readily computed in perturbation theory and this calculation is underway.

The second correction comes from residual taste-exchange interactions, which from the data in Fig. 7 could be of order a few MeV. Both this error and that corrected by $\delta\mathcal{L}_{\rm hfs}$ are approximately proportional to $a^2$. So we can estimate them (together) by comparing to a calculation with a different lattice spacing. We repeated our hyperfine splitting analysis on the $1/8$ fm lattice using the tuned $\epsilon(= -.21)$. The $a^2$ errors should be a little more than twice as large on the coarser lattice since $a^2$ is almost exactly twice as large. We obtained a splitting of 110(3) MeV on the coarse lattice, which is essentially identical to the 109(3) MeV we obtained on the fine lattice. Combining these results, together with our *a priori* expectation of $\pm 5$ MeV errors from $a^2$ corrections, we obtain an $a^2$ corrected hyperfine splitting is 109(5) MeV.

The third correction is due to the fact that our simulation does not include effects from the annihilation of the valence $c\bar{c}$ quarks into two or more gluons. Such annihilations are responsible for small shifts in the $\eta_c$ and $\psi$ masses, as well as for the (nonelectromagnetic) hadronic decay rate of each meson. The dominant contribution comes from $c\bar{c} \to gg$ and affects only the $\eta_c$. The shift in the $\eta_c$ energy is proportional to the perturbative amplitude for $c\bar{c} \to gg \to c\bar{c}$ at threshold [28] and therefore [29]

$$\Delta E_{\eta_c} - i\Gamma(\eta_c \to \text{hadrons})/2 \propto \ln(2) - 1 - i\frac{\pi}{2} + \mathcal{O}(\alpha_s). \tag{44}$$

This result implies that the leading correction to the $\eta_c$ mass due to $c\bar{c}$ annihilation can be computed from the hadronic width:

$$\begin{aligned}\Delta E_{\eta_c} &= \Gamma(\eta_c \to \text{hadrons})\left(\frac{\ln(2) - 1}{\pi} + \mathcal{O}(\alpha_s)\right) \\ &= -2.4(8)\ \text{MeV},\end{aligned} \tag{45}$$

where we use experimental results from [27]. This correction increases our theoretical value for the $\psi - \eta_c$ splitting to 111(5) MeV, which agrees well with the experiment.

The sea-quark masses in our simulations are not quite correct, but both theoretical expectations and experience with previous simulations indicate that this has negligible effect on this hyperfine splitting. We redid the analysis described above with the $u/d$ mass doubled, and confirmed that this is the case to our current level of precision.

This level of precision would be impossible using our ASQTAD results because the taste-exchange errors are tens of MeV—much larger than the $\pm 5$ MeV expected from other $a^2$ errors. This example confirms that taste-exchange errors are likely the dominant source of $a^2$ errors in the ASQTAD formalism. With HISQ, on the other hand, taste-exchange errors have been suppressed to a level commensurate with other errors.

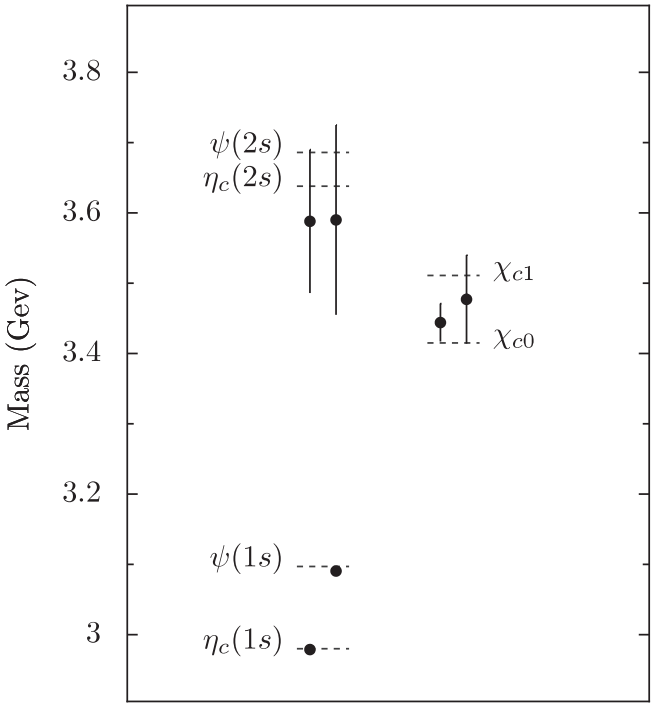


FIG. 8. Masses for different excitations of the $\psi$ meson from a simulation at lattice spacing $1/11$ fm. The dashed lines indicate the results from the experiment.

Finally we also computed the masses of some radially and orbitally excited states in the $\psi$ family using HISQ, although not as accurately as the ground-state masses. High-precision determinations of excited-state masses require careful design of the meson sources and sinks used in the simulation. Here we did not attempt high precision, but rather used simple local sources to do a quick check on the spectrum. Our results, shown in Fig. 8, agree well with the experiment to within our statistical errors.

## VI. SIMULATION TECHNIQUES FOR HIGHLY SMEARED OPERATORS

It would be highly desirable to create new unquenched gluon configurations using the HISQ action in place of the ASQTAD action. The use of such configurations, with lattice spacings of order $a = 0.1$ fm, would significantly reduce any residual worries about errors due to taste-exchange interactions.

Such simulations are complicated, however, by the heavily smeared, reunitarized links in the action. The additional smearing and reunitarization have no effect on the cost of the quark-matrix inversions required when updating gluon configurations, but they complicate calculation of the derivative $D_a(x, \mu)S_q$ of the quark action $S_q[U]$ with respect to an individual link operator $U_\mu(x)$. Derivative $D_a(x, \mu)$ is defined by

$$f(e^{i\epsilon^a T^a} U_\mu(x)) \equiv f(U_\mu(x)) + \epsilon^a D_a(x, \mu) f(U_\mu) + \mathcal{O}(\epsilon^2) \tag{46}$$

for any function $f$ of $U_\mu(x)$. We developed and tested both an analytic and a stochastic version of the derivative for this action [30].

The analytic version employs a unitary projection

$$V \longrightarrow (VV^\dagger)^{-(1/2)} V \tag{47}$$

to reunitarize each smeared link $V$. The main obstacle is then computation of the gauge derivative of the inverse square root. Using the product-rule identity for the matrix $M \equiv VV^\dagger$,

$$\begin{aligned} &M^{1/2}(DM^{-(1/2)}) + (DM^{-(1/2)})M^{1/2} \\ &\quad = -M^{-(1/2)}(DM)M^{-(1/2)}, \end{aligned} \tag{48}$$

we can solve for $D(VV^\dagger)^{-(1/2)}$ directly, both iteratively by the conjugate gradient algorithm, and exactly by first diagonalizing $VV^\dagger$.

Using the chain rule, we combine $D(VV^\dagger)^{-(1/2)}$ with standard derivatives of the base action and of the smeared links $V$. We encode derivatives of the action and smeared links generically, allowing for run-time changes independently in either. The additional cost of computing and combining $D(VV^\dagger)^{-(1/2)}$ with these is minimal.

Several other analytic approaches have been developed for unitarized smearings [31,32]. The authors of [31] addressed the problem of computing the derivative of the matrix inverse square root by replacing it with a rational approximation. In [32], the smearing itself is unitary, explicitly avoiding the need to reunitarize and the inverse square root. In both, the derivatives are then computed straightforwardly.

In the stochastic approach, we define links

$$U_\mu^\eta(x) \equiv e^{i\epsilon\eta(x,\mu)} U_\mu(x), \tag{49}$$

where $\eta(x, \mu)$ is now a field of traceless, Hermitian $3 \times 3$ random matrices, each with normalization

$$\langle \eta_{ij} \eta_{lm} \rangle_\eta = (\delta_{im}\delta_{jl} - \tfrac{1}{3}\delta_{ij}\delta_{lm}), \tag{50}$$

and $\epsilon$ is a very small number. Defining $\Delta S_q(x, \mu)$ to be the terms in $S_q[U^\eta] - S_q[U]$ containing $U_\mu(x)$, the derivative can be computed efficiently from

$$2\epsilon T^a D_a(x, \mu) S_q \approx \langle \eta(x, \mu) \Delta S_q(x, \mu) \rangle_\eta \tag{51}$$

averaged over a finite number of sets of random $\eta$s. Our numerical experiments suggest that 10–100 sets of $\eta$s are adequate for actions like HISQ. We will describe both our stochastic and analytic techniques in a later paper.

## VII. CONCLUSIONS

In this paper, we have demonstrated that taste-exchange interactions are perturbative and we have shown how to use Symanzik improvement to create a new staggered-quark action (HISQ) that has greatly reduced one-loop taste-exchange errors, no tree-level order $a^2$ errors, and no tree-level order $(am)^4$ errors to leading order in the quark's velocity $v/c$. The HISQ action addresses one of the fundamental issues surrounding staggered-quark simulations by allowing us to estimate taste-exchange interactions through comparisons of HISQ with ASQTAD results. We presented numerical evidence that taste-exchange interactions in HISQ contribute less than 1% to light-quark quantities, like meson masses and decay constants, at lattice spacings as large as 0.1 fm.

The suppression of all order $(am)^4$ errors by powers of $(v/c)^2$ makes HISQ the most accurate discretization of the quark action for simulating $c$ quarks on current lattices. We demonstrated this with a new lattice QCD determination of the $\psi - \eta_c$ mass splitting, which agrees well with the experiment. This result could be improved by computing the coefficient $c_{\rm hfs}$ in the correction $\delta\mathcal{L}_{\rm hfs}$ (Eq. (43)) to the HISQ action.

Our final HISQ action is defined by Eqs. (37)–(40). We showed that the tree-level value (Eq. (24)) for the Naik-term parameter $\epsilon$ is adequate at the level of 1% errors for lattice spacings at least as large as $1/8$ fm.

The HISQ formalism will be most useful for $D$ physics and works very well for such mesons. In Fig. 9, for example, we show the $D_s^* - D_s$ spin splitting from simulations with HISQ $c$ quarks using both our $1/8$ fm and

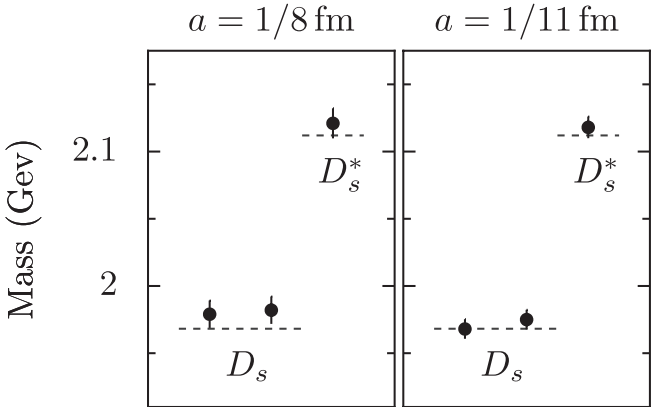


FIG. 9. Masses for two different tastes of the $D_s$ and one for the $D_s^*$ using HISQ $c$ quarks on lattices with lattice spacings $a = 1/8$ fm ($\epsilon = -0.21$) and $1/11$ fm ($\epsilon = -0.115$). For HISQ, $D_s$s are given (from left to right) for the 0-link and 1-temporal-link mesons; only the 0-link splitting is given for the $D_s^*$. The dashed lines indicate the results from the experiment. The error bars shown are from the simulated values for $m_{D_s} - m_{\eta_c}/2$ and $m_{D_s^*} - m_{\eta_c}/2$, since these quantities are insensitive to the $c$ mass and the $c$ mass was tuned to make the simulated value for $m_{\eta_c}$ exact.

$1/11$ fm lattices. As in the charmonium case, theory and experiment agree well here to within errors. Another very sensitive test of our simulations is to compare computed and experimental values for the mass difference $2m_{D_s} - m_{\eta_c}$, which is quite insensitive to tuning errors in the $c$ mass. We obtain 956(14) MeV using HISQ on the $1/11$ fm lattice, and 978(20) MeV on the $1/8$ fm lattice. Both values agree well with the splitting 956(1) MeV from the experiment. Finally, we measured the speed of light and found $c^2 = 1.00(4)$ for the $D_s$ on the coarse lattice ($a = 1/8$ fm with $\epsilon = -0.21$), confirming that the same action, with the same values for the coupling constants, works for both $D_s$ and $\eta_c$ mesons. It is important to appreciate that there are no free parameters available for tuning in the extraction of any of these results; all QCD parameters were tuned using other quantities.

As we will discuss in a later paper, the HISQ formalism is particularly useful for accurate calculations of quantities like $f_D$, $f_{D_s}$, $D \to \pi l \nu$, and so on. These all require currents and these currents, even though they are conserved or partially conserved, have order $\alpha_s(am)^2$ renormalizations. Consider, for example, $c\bar{c}$ annihilation into a (virtual) photon. The electromagnetic current can be computed by inserting photon link operators,

$$U_\mu^{\mathrm{QED}} \equiv \exp\left(-ie_q \int_x^{x+\hat{\mu}} dx \cdot A^{\mathrm{QED}}\right), \tag{52}$$

into the HISQ action and then expanding to first order in $A^{\mathrm{QED}}$ to obtain

$$-ie_q A_\mu^{\mathrm{QED}} J_\mu^{\mathrm{QED}}. \tag{53}$$

Current $J^{\mathrm{QED}}$ is not renormalized, because of QED's gauge symmetry, but it is not the only operator that contributes to $c\bar{c}$ annihilation. In addition there are $\mathcal{O}(a^2)$ correction terms that contribute,

$$c_1 \alpha_s a^2 m \bar{\psi} \sigma \cdot e_q F^{\mathrm{QED}} \psi + c_2 \alpha_s a^2 \bar{\psi} (D \cdot e_q F)^{\mathrm{QED}} \cdot \gamma \psi, \tag{54}$$

just as for the gluon fields. The first correction term renormalizes the quark's magnetic moment, the second its charge radius. Such terms are normally negligible since the extra derivatives introduce extra powers of $(ap)^2$ and $p$ is small. For $c$ quark annihilations, however, the extra derivatives become $c$ quark masses instead of small momenta, and so are more important. It is easy to compute coefficients $c_1$ and $c_2$ in perturbation theory, but contributions to annihilation from these operators are indistinguishable from those coming from the leading operator $J^{\mathrm{QED}}$. Consequently we can omit the corrections and, instead, introduce a renormalization constant for $J^{\mathrm{QED}}$:

$$J_\mu^{\mathrm{QED,continuum}} = Z_{\mathrm{eff}} J_\mu^{\mathrm{QED,HISQ}}, \tag{55}$$

where

$$Z_{\mathrm{eff}} = 1 + c\alpha_s(am)^2 + \mathcal{O}(\alpha_s^2(am)^2). \tag{56}$$

The situation is very similar for (partially conserved) weak-interaction currents. Again the current derived from the action requires $\mathcal{O}(\alpha_s(am)^2)$ corrections. Once these one-loop corrections have been calculated and included, however, the remaining terms are only $\mathcal{O}(\alpha_s^2(am)^2)$. Consequently one-loop radiative corrections are all that is necessary to achieve 1%–2% precision for $f_D$, $D \to \pi l \nu$, and similar quantities. Other discretization errors in these quantities should be of order 1% or less. With one-loop renormalizations, lattice results will be more accurate than current results from CLEO-c and the $b$ factories.

## ACKNOWLEDGMENTS

We thank the MILC collaboration for sharing their configurations with us. This work was funded by grants from the NSF, DOE, and PPARC. The calculations were carried out on computer clusters at Scotgrid and QCDOCX; we thank David Martin and EPCC for assistance.

## APPENDIX A: GAMMA MATRICES

The complete set of spinor matrices can be labeled by a four-component vector $n_\mu$ consisting of 0s and 1s (i.e., $n_\mu \in \mathbb{Z}_2$):

$$\gamma_n \equiv \prod_{\mu=0}^{3} (\gamma_\mu)^{n_\mu}. \tag{A1}$$

We will also sometimes use the more conventional, but equivalent (up to a phase) Hermitian set:

1, $\gamma_5 \equiv \gamma_t\gamma_x\gamma_y\gamma_z$, $\gamma_\mu$, $\gamma_{5\mu} \equiv i\gamma_5\gamma_\mu$, $\gamma_{\mu\nu} \equiv \frac{i}{2}[\gamma_\mu, \gamma_\nu]$. (A2)

The $\gamma_n$s have several useful properties:

(i) orthonormal:

$$\mathrm{Tr}\,(\gamma_n^\dagger\gamma_m) = 4\delta_{nm}, \tag{A3}$$

(ii) closed under multiplication:

$$\gamma_n\gamma_m = (-1)^{n\cdot m^<}\gamma_{n+m}, \tag{A4}$$

where

$$m_\mu^< \equiv \sum_{\nu<\mu} m_\nu \bmod 2 \tag{A5}$$

and

$$n\cdot m^< = n^>\cdot m \tag{A6}$$

with

$$n_\mu^> \equiv \sum_{\nu>\mu} n_\nu \bmod 2; \tag{A7}$$

(iii) Hermitian or anti-Hermitian:

$$\gamma_n^\dagger = (-1)^{n\cdot n^<}\gamma_n = \gamma_n^{-1}; \tag{A8}$$

(iv) commuting or anticommuting:

$$\gamma_n\gamma_m = (-1)^{\bar m\cdot n}\gamma_m\gamma_n, \tag{A9}$$

where

$$\bar m_\mu \equiv m_\mu^> + m_\mu^< = \sum_{\nu\neq\mu} m_\nu \bmod 2 = \begin{cases} m_\mu & \text{if } m^2 \text{ even} \\ (m_\mu + 1) \bmod 2 & \text{if } m^2 \text{ odd,} \end{cases} \tag{A10}$$

and

$$\bar m\cdot n = \bar n\cdot m, \tag{A11}$$

$$\bar{\bar m} = m \qquad (\bar m\cdot m) \bmod 2 = 0; \tag{A12}$$

(v) permutation operator: if one uses the standard representation for gamma matrices, where

$$\gamma_0 = \begin{pmatrix} 1 & 0 \\ 0 & -1 \end{pmatrix}, \qquad \gamma_i = \begin{pmatrix} 0 & \sigma_i \\ \sigma_i & 0 \end{pmatrix}, \tag{A13}$$

and

$$\sigma_1 = \begin{pmatrix} 0 & 1 \\ 1 & 0 \end{pmatrix}, \qquad \sigma_2 = \begin{pmatrix} 0 & -i \\ i & 0 \end{pmatrix}, \qquad \sigma_3 = \begin{pmatrix} 1 & 0 \\ 0 & -1 \end{pmatrix}, \tag{A14}$$

then there is at most one nonzero element in any row or any column of any $\gamma_n$, and that element is $\pm 1$ or $\pm i$. Thus multiplying a spinor $\psi$ by $\gamma_n$ simply permutes the spinor components of $\psi$, multiplying each by $\pm 1$ or $\pm i$.

A convenient notation, reminiscent of $\gamma_{5\mu}$, is

$$\gamma_{nm} \equiv \gamma_n\gamma_m. \tag{A15}$$

## APPENDIX B: STAGGERED QUARKS

The naive discretization of the quark action is formally equivalent to the staggered-quark discretization. Staggering is an important optimization in simulations; it is also a remarkable property. Consider the following local transformation of the naive-quark field:

$$\psi(x) \to \Omega(x)\chi(x), \qquad \bar\psi(x) \to \bar\chi(x)\Omega^\dagger(x), \tag{B1}$$

where

$$\Omega(x) \equiv \gamma_x \equiv \prod_{\mu=0}^{3}(\gamma_\mu)^{x_\mu}, \tag{B2}$$

and we have set the lattice spacing $a = 1$ for convenience. (We will use lattice units, where $a = 1$, in this and all succeeding appendices.) Note that

$$\Omega(x) = \gamma_n \qquad \text{for } n_\mu = x_\mu \bmod 2; \tag{B3}$$

there are only 16 different $\Omega$s. It is easy to show that

$$\alpha_\mu(x) \equiv \Omega^\dagger(x)\gamma_\mu\Omega(x \pm \hat\mu) = (-1)^{x_\mu^<}, \tag{B4}$$

$$1 = \Omega^\dagger(x)\Omega(x), \tag{B5}$$

where $x_\mu^< \equiv x_0 + x_1 + \cdots + x_{\mu-1}$ (see Appendix A). Therefore the naive-quark action can be rewritten

$$\bar\psi(x)(\gamma\cdot\Delta + m)\psi(x) = \bar\chi(x)(\alpha(x)\cdot\Delta + m)\chi(x). \tag{B6}$$

Remarkably the $\chi$ action is diagonal in spinor space; each component of $\chi$ is exactly equivalent to every other component. Consequently the $\chi$ propagator is diagonal in spinor space in *any background gauge field*:

$$\langle\chi(x)\bar\chi(y)\rangle_\chi = s(x, y)\mathbf{1}_{\text{spinor}}, \tag{B7}$$

where $s(x, y)$ is the one-spinor-component staggered-quark propagator. Transforming back to the original naive-quark field we find that

$$S_F \equiv \langle\psi(x)\bar\psi(y)\rangle_\psi = s(x, y)\Omega(x)\Omega^\dagger(y). \tag{B8}$$

This last result is a somewhat surprising consequence of the doubling symmetry. It says that the spinor structure of the naive-quark propagator is completely independent of the gauge field. This is certainly not the case for individual tastes of naive quark, whose spins will flip back and forth as they scatter off fluctuations in the chromomagnetic field, for example. The 16 tastes of the naive-quark field are

packaged in such a way, however, that all gauge-field dependence vanishes in the spinor structure.

Doubling symmetry is immediately evident in the staggered action, Eq. (B6), since the action is invariant under

$$\chi(x) \to \mathcal{B}_\zeta(0)\chi(x), \tag{B9}$$

which merely scrambles the (equivalent) spinor components of $\chi(x)$, and since

$$\mathcal{B}_\zeta(x)\Omega(x) = \Omega(x)\mathcal{B}_\zeta(0). \tag{B10}$$

In simulations one generally discards all but one spinor component of $\chi(x)$, resulting in highly efficient algorithms. The Symanzik improvements discussed above are trivially incorporated.

Note, finally, that Eq. (B10) implies

$$\mathcal{B}_\zeta(x)\Omega(x)\Omega^\dagger(y)\mathcal{B}_\zeta^\dagger(y) = \Omega(x)\Omega^\dagger(y) \tag{B11}$$

and therefore the naive-quark propagator $S_F$ satisfies

$$S_F(x, y) = \mathcal{B}_\zeta(x)S_F(x, y)\mathcal{B}_\zeta^\dagger(y) \tag{B12}$$

for any background gauge field. In momentum space this becomes

$$S_F(p, q) = \mathcal{B}_\zeta(0)S_F(p + \zeta\pi, q + \zeta\pi)\mathcal{B}_\zeta^\dagger(0), \tag{B13}$$

which is an exact relationship that is useful in perturbative calculations. This last relation, which is easily checked at tree level (but true to all orders in $\alpha_s$), shows that there is only one 16th as much information in the naive-quark propagator as naively expected.

## APPENDIX C: TASTE, NAIVE VS. STAGGERED

The quark field $\psi(x)$ will typically contain contributions from all 16 tastes. One can separate out (approximately) the different tastes by blocking the field on hypercubes that have two sites per side. One way to project out the $\zeta = 0$ taste, for example, is to average over the hypercube:

$$\psi_B = \frac{1}{16}\sum_{\delta x_\mu \in \mathbb{Z}_2} \psi(x_B + \delta x), \tag{C1}$$

where $x_B$, with $x_{B\mu} \bmod 2 = 0$, identifies the hypercube, and the sum is over all 16 sites in the hypercube. We are ignoring gluons here, for simplicity. Any component of $\psi(x)$ that has momentum $p \approx \zeta\pi$ with $\zeta \neq 0$ will be strongly suppressed by the average: the suppression factor is $\mathcal{O}(ap)$ for a mode with momentum $p + \zeta\pi$, and so vanishes only in the continuum limit. A $\zeta \neq 0$ component of the original field $\psi(x)$ can be isolated by applying a doubling operator $\mathcal{B}_\zeta$ to transform that component to $\zeta = 0$, and then, again, averaging over the hypercube to isolate $\zeta = 0$:

$$\psi_B^{(\zeta)} = \frac{1}{16}\sum_{\delta x_\mu \in \mathbb{Z}_2} \mathcal{B}_\zeta(x_B + \delta x)\psi(x_B + \delta x). \tag{C2}$$

The 16 blocked fields $\psi_B^{(\zeta)}$, with one for each $\zeta$, describe the 16 different tastes of quark, each now in the low-momentum sector (i.e., with $p_\mu \leq \pi/2$). Here $\zeta$ labels the corner of the original field's Brillouin zone ($p \approx \zeta\pi$) that corresponds to the blocked field.

With staggered quarks, one keeps only one component of $\chi(x)$ since the components are equivalent and decouple:

$$\chi(x) \to \begin{bmatrix} \chi_1(x) \\ 0 \\ 0 \\ 0 \end{bmatrix}. \tag{C3}$$

We can use our hypercube blocking (Eq. (C2)) to translate this single field back into blocked fields for "ordinary" quarks of different tastes $\zeta$:

$$\sum_{\delta x_\mu \in \mathbb{Z}_2} \mathcal{B}_\zeta(x_B + \delta x)\psi(x_B + \delta x) = \sum_{\delta x} \Omega(\delta x)\mathcal{B}_\zeta(0) \begin{bmatrix} \chi_1(x_B + \delta x) \\ 0 \\ 0 \\ 0 \end{bmatrix}. \tag{C4}$$

Only four of the 16 blocked fields are independent, however, because $\mathcal{B}_\zeta(0)\chi(x)$ is always proportional to one of only four different spinors:

$$\begin{bmatrix} \chi_1(x) \\ 0 \\ 0 \\ 0 \end{bmatrix}, \begin{bmatrix} 0 \\ \chi_1(x) \\ 0 \\ 0 \end{bmatrix}, \begin{bmatrix} 0 \\ 0 \\ \chi_1(x) \\ 0 \end{bmatrix}, \begin{bmatrix} 0 \\ 0 \\ 0 \\ \chi_1(x) \end{bmatrix}. \tag{C5}$$

(This is because $\mathcal{B}_\zeta(0) = \gamma_{\bar{\zeta}}$ and all $\gamma_n$s when applied to a spinor merely permute the elements of the spinor, multiplying each by $\pm 1$ or $\pm i$.) Consequently we can reconstruct just four tastes, $t = 1 \ldots 4$, of blocked quark from a single staggered field:

$$\tilde{\psi}_B^{(t)} = \sum_{\delta x} \Omega(\delta x)\hat{\chi}^{(t)}\chi_1(x_B + \delta x), \tag{C6}$$

where the $\hat{\chi}^{(t)}$ are unit spinors with $\hat{\chi}_i^{(t)} = \delta_{i,t}$. This formula defines the standard blocked-field flavor basis for staggered quarks [33].

Formula (C4) shows that some $\zeta$'s become indistinguishable in the staggered approximation. In fact, by explicit calculation (given our specific representation of the $\gamma$ matrices), one finds that the $\zeta$s fall into four equivalence classes composed of indistinguishable $\zeta$s:

| | | | | |
|---|---|---|---|---|
| $A$: | 0000 | 0001 | 0110 | 0111 |
| $B$: | 0010 | 0011 | 0100 | 0101 |
| $C$: | 1000 | 1001 | 1110 | 1111 |
| $D$: | 1010 | 1011 | 1100 | 1101 |

(C7)

These four classes correspond to the four tastes of staggered quark; all the $\zeta$s in a single class give the same staggered-quark field $\tilde{\psi}_B^{(t)}$ (Eq. (C6)) from Eq. (C4).

The equivalence of the $\zeta$s within a single class is preserved under addition of $\zeta$s; for example, adding any two $\zeta$s from class $B$ always gives a $\zeta$ in class $A$, while adding any vector from class $B$ to any vector from class $C$ always gives a vector in class $D$. The full addition table for these classes is:

| + | $A$ | $B$ | $C$ | $D$ |
|---|---|---|---|---|
| $A$ | $A$ | $B$ | $C$ | $D$ |
| $B$ | $B$ | $A$ | $D$ | $C$ |
| $C$ | $C$ | $D$ | $A$ | $B$ |
| $D$ | $D$ | $C$ | $B$ | $A$ |

This kind of structure is necessary for the fourfold reduction in the number of tastes due to staggering—that is, 16 tastes of naive quark are reduced to 4 tastes of staggered quark because we can consistently identify certain corners of the Brillouin zone with each other in the staggered case.

We note finally, for this section, that the naive-quark action (and improved versions of it) can be rewritten in terms of the flavor-basis blocked fields defined in Eq. (C2) by substituting the inverse of that equation,

$$\psi(x_B + \delta x) = \sum_\zeta \mathcal{B}^\dagger_\zeta(x_B + \delta x)\psi^{(\zeta)}_B, \tag{C8}$$

into the action. The staggered-quark version of the resulting blocked-field action is frequently presented in pedagogical presentations of staggered quarks [33]. Such blocked actions are not so useful for applications, however, in part because of the complexity of including gauge fields. And they are particularly misleading when analyzing finite-$a$ errors, as we do in this paper. This is because, as noted above, one can only isolate different tastes up to corrections of $\mathcal{O}(a)$ when averaging on a $2^4$ hypercube. Consequently, the blocked field for a given taste (Eq. (C2)) is contaminated by other tastes in $\mathcal{O}(a)$, and the action for that blocked field must have $\mathcal{O}(a)$ terms that violate taste symmetry, even for noninteracting quarks. These $\mathcal{O}(a)$ terms, which are discussed in [33], apparently contradict our assertion that taste changes arise only through hard-gluon exchanges, which appear only in $\mathcal{O}(a^2)$ and higher. The $\mathcal{O}(a)$ terms in the blocked action are, however, entirely an artifact of the definition of the blocked fields; they are *not* a property of the underlying theory and cannot affect physical results. Indeed it is obvious from the naive-quark formalism that there can be no $\mathcal{O}(a)$ errors of any sort since there are no dimension-5 operators in that formalism (see Table III) that are consistent with the chiral, gauge, and other symmetries of the theory [34].

The $a^n$ errors are most easily understood in the original naive-quark formalism, using momentum space to sort out the different tastes, each of which corresponds to a different corner of the Brillouin zone. Contrary to what happens in the blocked-field actions, there can be no violations of taste symmetry in the free naive-quark theory, because of momentum conservation [33]. All taste changes must involve exchange of hard gluons ($q_{\rm tot} \approx \zeta\pi/a$ for $\zeta_\mu \in \mathbb{Z}_2$) between two or more quark lines—and therefore are $\mathcal{O}(a^2)$ or higher. Working in momentum space is also particularly convenient for the matching calculations needed for Symanzik improvement, and, as we show in the next section, there is no practical need for the blocked-field formalisms.

## APPENDIX D: NAIVE-QUARK CURRENTS

Naive quarks lead to huge numbers of nearly equivalent mesons. Where in ordinary QCD one might consider a single meson operator, $J_n = \bar\psi\gamma_n\psi$, one has 16 point-split operators in the naive theory each of which couples to a different meson:

$$\begin{aligned} J^{(s)}_n(x) &\equiv \bar\psi(x)\gamma^{(s)}_n\psi(x) \equiv \bar\psi(x)\gamma_n\psi(x + \delta x_{sn}) \\ &\propto \bar\chi(x)\gamma_s\chi(x + \delta x_{sn}), \end{aligned} \tag{D1}$$

where $s$ is any one of the 16 four-vectors consisting of 0s and 1s only,

$$\delta x_{sn} \equiv (s + n) \bmod 2, \tag{D2}$$

and link operators $U_\mu$ are implicit (and $a = 1$ still). Each of these operators creates a different version of the $J_n$ meson; they are orthogonal. This is because

$$J^{(s)}_n \to (-1)^{s_\mu} J^{(s)}_n \tag{D3}$$

under a doubling transformation where

$$\psi(x) \to \mathcal{B}_{\zeta=\hat\mu}(x)\psi(x), \qquad \bar\psi(x) \to \bar\psi(x)\mathcal{B}^\dagger_{\hat\mu}(x). \tag{D4}$$

Thus the four-vector $s$ determines the bilinear's transformation properties under arbitrary doubling transformations; it specifies the bilinear's "signature" under doubling transformations. Since doubling transformations are symmetries of the naive theory, the doubling signature is conserved; for example,

$$\langle J^{(r)}_m J^{(s)\dagger}_n\rangle = 0 \quad \text{if } r \neq s, \tag{D5}$$

which proves that each of our point splittings creates a different meson.

Different signatures correspond to different variations of the same continuum meson, typically with slightly different masses, etc. These are the different tastes of the meson. We label different tastes by the corresponding signature $s$ in the meson's rest frame.

Additional mesons are made by boosting particles into other corners of the Brillouin zone:

$$p_{\rm tot} \approx \zeta\pi \tag{D6}$$

for one of the 16 $\zeta$s. Such mesons would be highly relativistic in the continuum, but here they are equivalent to low-energy mesons because of the doubling symmetry; for example, the antiquark in the meson might carry a momentum near zero, while the quark carries $\zeta\pi$ but is then

equivalent to a zero-momentum quark state through the doubling symmetry. Pushing such momenta through a naive-quark bilinear, using for example

$$\sum_x e^{ip_{\rm tot}\cdot x} J_n^{(s)}(x), \tag{D7}$$

changes the quantum numbers of the meson created by the operator. To see this, consider current

$$J_n^{(\zeta,s)}(x) \equiv (-1)^{\zeta\cdot x}\bar\psi(x)\gamma_\zeta^\dagger\gamma_n^{(s)}\psi(x) = \bar\psi(x)\mathcal{B}_\zeta^\dagger(x)\gamma_n^{(s)}\psi(x) \tag{D8}$$

$$\propto \bar\chi(x)\gamma_\zeta^\dagger\gamma_s\chi(x+\delta x_{sn}) \tag{D9}$$

which has signature $(\bar\zeta + s) \bmod 2$. This current obviously carries momentum $p_{\rm tot} = \zeta\pi$ if averaged over all $x$. It is easy to show that flavor-nonsinglet mesons created by $J_n^{(\zeta,s)}$ with different $\zeta$s are all identical, and therefore all carry taste $s$. For a $\bar u d$ meson, for example, we can use the *separate* doubling symmetries of the $u$ and $d$ to prove that

$$\begin{aligned}\langle J_n^{(\zeta,s)}(x)J_n^{(\zeta,s)\dagger}(y)\rangle &\equiv \langle \bar u\mathcal{B}_\zeta^\dagger\gamma_n^{(s)}d\bar d\gamma_n^{(s)}\mathcal{B}_\zeta u\rangle \\ &= \langle \bar u\gamma_n^{(s)}d\bar d\gamma_n^{(s)}u\rangle \equiv \langle J_n^{(s)}(x)J_n^{(s)\dagger}(y)\rangle\end{aligned} \tag{D10}$$

for all $\zeta$s.

The labeling on $J_n^{(\zeta,s)}$ is intuitive (and therefore useful) only if the current is averaged over $x$ in such a way that $p_{\rm tot} = \zeta\pi + p$ where $-\pi/2 < p_\mu \le \pi/2$ for all $\mu$; the combination of all $\zeta$s and $p$s covers all of momentum space, so nothing is lost by this restriction and double counting is avoided. We can enforce this restriction on the momenta by redefining the current on a blocked lattice with one site at the center of every $2^4$ hypercube on the original lattice, just as we did for the quark field (Appendix C):

$$J_{Bn}^{(\zeta,s)} \equiv \sum_{\delta x_\mu\in\mathbb{Z}_2} J_n^{(\zeta,s)}(x_B + \delta x), \tag{D11}$$

where $x_B$ identifies the hypercube (with $x_{B\mu} \bmod 2 = 0$). The blocked current creates a meson of taste $s$ with momentum in the $\zeta\pi$ corner of the Brillouin zone.

Note that momentum and taste conservation imply

$$\sum_{x,y}\langle J_n^{(\zeta,s)}(x)J_n^{(\zeta',s')\dagger}(y)\rangle = 0 \tag{D12}$$

unless $\zeta = \zeta'$ and $s = s'$. Consequently the different operators are orthogonal when analyzed in momentum space. Typically we sum over space, however, but not time. In that case operators with the same signature, but where $\zeta' - \zeta = \pm\hat t$, can mix. This mixing leads to components in meson propagators that oscillate in time, as we discuss below.

To summarize, there are 16 sets, each set labeled by taste $s$, of 16 identical mesons, each meson labeled by $\zeta$, for each flavor-nonsinglet meson in the continuum. Each corner $\zeta$ of the Brillouin zone has a single representative of each taste of meson.

Flavor-singlet mesons are slightly more complicated. In a $\bar uu$ meson, for example, the quark and antiquark are created by the same field, and so do not have separate doubling transformations. Therefore the argument relating $J_n^{(\zeta,s)}$s with different $\zeta$s does not work. The only contributions that spoil this argument are from annihilation, where the meson's quark and antiquark annihilate into gluons. Annihilation gluons that contribute to, for example,

$$\sum_{\vec x}\langle J_n^{(\zeta,s)}(x)J_n^{(\zeta,s)\dagger}(0)\rangle \tag{D13}$$

carry total momentum $\zeta\pi$ and so are far off shell unless $\zeta = 0$. This has two implications: First, annihilation contributions will be different for different $\zeta$s. And, second, only the $\zeta = 0$ case has the correct coupling between the flavor-singlet quarks and purely gluonic channels. In fact, only the taste-singlet state, among the $\zeta = 0$ states, couples to the gluons since

$$\langle J_n^{(s)}(x)\rangle_\psi \propto {\rm Tr}(\gamma_s) = 0 \quad \text{unless } s = 0. \tag{D14}$$

A similar condition applies to nonzero $\zeta$s as well. For each $\zeta$ there is only one taste that can couple to gluons. The gluons are highly virtual if $\zeta$ is nonzero. These last contributions are taste violating because they change quark taste along quark lines; they are removed by the contact terms discussed in this paper.

It is not surprising that the flavor-singlet mesons are more complicated. They usually have to be, particularly in the pseudoscalar channel where the $U(1)$ problem must be resolved. In our naive-quark theory, only the $\zeta = s = 0$ mesons couple properly to gluons. The masses of pseudoscalars with $\zeta = s = 0$ are shifted properly by instantons in the chiral limit, so that the $U(1)$ problem is resolved. The $\zeta = s = 0$ neutral pion is also the only pion that decays to two photons. The corresponding axial-vector current is only approximately conserved, even in the chiral limit, so anomalies are not needed to mediate the photon decay.

## APPENDIX E: STAGGERED-QUARK CURRENTS

The 256 different mesons created by the naive-quark bilinears $J_n^{(\zeta,s)}$ include 16 identical copies of each distinct taste of meson. Staggering the quark fields discards identical copies, leaving just 16 distinct tastes. The naive-quark bilinears corresponding to the staggered-quark bilinears are the ones that become diagonal after they are staggered. Any other operator creates mesons that mix different spinor components of the staggered-quark operator $\chi(x)$ (Eq. (B1)), and so is discarded when we stagger.

We can identify the bilinears that survive staggering by noting that

$$J_n^{(\zeta,s)} \propto \bar{\chi}\gamma_{\tilde{\zeta}}^{\dagger}\gamma_s\chi \to \bar{\chi}\chi \tag{E1}$$

after staggering provided $\zeta = \bar{s}$. The staggered-quark operator is therefore

$$\begin{aligned} J_n^{(\bar{s},s)} &\equiv (-1)^{\bar{s}\cdot x}\bar{\psi}(x)\gamma_s^{\dagger}\gamma_n\psi(x+\delta x_{sn}) \\ &= \beta_n^{(s)}(x)\bar{\chi}(x)\chi(x+\delta x_{sn}), \end{aligned} \tag{E2}$$

where again $\delta x_{sn} = (s+n) \bmod 2$ (with $a = 1$), and

$$\begin{aligned} \beta_n^{(s)}(x) &= \tfrac{1}{4}\mathrm{Tr}(\gamma_s^{\dagger}\gamma_x^{\dagger}\gamma_n\gamma_{x+s+n}) \\ &= (-1)^{x\cdot(s^{<}+n^{>})}(-1)^{n\cdot(s+n)^{<}}. \end{aligned} \tag{E3}$$

Each taste $s$ in the staggered theory corresponds to a specific corner of the Brillouin zone, with $p_{\mathrm{tot}} \approx \bar{s}\pi$, in the naive-quark theory. These operators have zero signature and so are unchanged under doubling transformations (Eq. (6)).

It is useful for formal analyses, though less so for simulations, to introduce a slightly different definition for these bilinears by defining a new operator on our naive-quark field:

$$\gamma_n \otimes \xi_s\psi(x) \equiv (-1)^{\bar{s}\cdot x}\gamma_s^{\dagger}\gamma_n\psi(x \oplus (n+s)), \tag{E4}$$

where $\oplus$ adds vector $n+s$ to $x$ "modulo" the hypercube that $x$ lies in—that is,

$$(x \oplus n)_\mu \equiv x_{B\mu} + (x_\mu - x_{B\mu} + n_\mu) \bmod 2 \tag{E5}$$

when $x$ is in the hypercube labeled by site $x_B$ (with $x_{B\mu} \bmod 2 = 0$). Thus $x \oplus n$ is in the same hypercube as $x$. With this definition, we can redefine the staggered-quark current with spin $n$ and taste $s$ to be:

$$\bar{\psi}(x)\gamma_n \otimes \xi_s\psi(x). \tag{E6}$$

The $\oplus$ means that the new operators $\gamma_n \otimes \xi_s$ have a simple algebra. If, for example,

$$\tilde{\psi}(x) \equiv \gamma_n \otimes \xi_s\psi(x) \tag{E7}$$

then, using Eq. (A9),

$$\gamma_m \otimes \xi_r\tilde{\psi}(x) = \gamma_m\gamma_n \otimes \xi_r\xi_s\psi(x), \tag{E8}$$

which implies that in general

$$\gamma_m \otimes \xi_r\gamma_n \otimes \xi_s = \gamma_m\gamma_n \otimes \xi_r\xi_s. \tag{E9}$$

Note that these definitions also imply that $\xi$s anticommute just as $\gamma$s; for example,

$$\gamma_n \otimes \xi_r\xi_s = (-1)^{\bar{r}\cdot s}\gamma_n \otimes \xi_s\xi_r. \tag{E10}$$

We can effectively restrict our current to the $\zeta = \bar{s}$ corner of the Brillouin zone by again blocking on $2^4$ hypercubes to obtain

$$\mathcal{J}_s^{(n)}(x_B) = \frac{1}{16}\sum_{\delta x_\mu \in \mathbb{Z}_2} \bar{\psi}(x_B+\delta x)\gamma_n \otimes \xi_s\psi(x_B+\delta x), \tag{E11}$$

where $x_{B\mu} \bmod 2 = 0$. This formula is related to a more standard formula by staggering the meson operator:

$$\bar{\psi}(x)\gamma_n \otimes \xi_s\psi(x) = \bar{\chi}(x)\gamma_s^{\dagger}\gamma_x^{\dagger}\gamma_n\gamma_{x+\delta x_{sn}}\chi(x \oplus \delta x_{sn}), \tag{E12}$$

where the shift $\delta x_{sn}$ guarantees that the product of $\gamma$s is proportional to the unit matrix. We can rewrite this in terms of a sum over $\delta x$s in the positive unit hypercube:

$$\sum_{\delta x_\mu \in \mathbb{Z}_2} \bar{\chi}(x)\frac{1}{4}\mathrm{Tr}(\gamma_s^{\dagger}\gamma_x^{\dagger}\gamma_n\gamma_{x+\delta x})\chi(x \oplus \delta x). \tag{E13}$$

Averaging over the hypercube gives a standard formula for $\mathcal{J}_s^{(n)}$:

$$\frac{1}{16}\sum_{\delta x, \delta x'} \bar{\chi}(x_B+\delta x)\frac{1}{4}\mathrm{Tr}(\gamma_s^{\dagger}\gamma_{\delta x}^{\dagger}\gamma_n\gamma_{\delta x'})\chi(x_B+\delta x'). \tag{E14}$$

Taste and spinor structure in $\bar{\psi}(x)\gamma_n \otimes \xi_s\psi(x)$ are both described by the same kind of four vector consisting of 0s and 1s. For this reason it is common practice to use the same terminology for describing taste as we do for spinor structure. Thus, for example, $\bar{\psi}(x)\gamma_5 \otimes \xi_5\psi(x)$ creates a pseudoscalar meson with "pseudoscalar taste." In this case $n = s = (1,1,1,1)$, and, from Eq. (E2),

$$\bar{\psi}(x)\gamma_5 \otimes \xi_5\psi(x) = \beta_5^{(5)}(x)\bar{\chi}(x)\chi(x) = (-1)^{x\cdot x}\bar{\chi}(x)\chi(x). \tag{E15}$$

A different pion is created by $\bar{\psi}(x)\gamma_5 \otimes \xi_{5\mu}\psi(x)$, this one with axial-vector taste:

$$\bar{\psi}(x)\gamma_5 \otimes \xi_{5\mu}\psi(x) = \beta_5^{(5\mu)}(x)\bar{\chi}(x)\chi(x \oplus \hat{\mu}). \tag{E16}$$

The pion created by this operator is sometimes called a $5 \otimes 5\mu$ or "1-link pion" since the operator is split by one link or lattice spacing. Similarly $\bar{\psi}(x)\gamma_5 \otimes \xi_5\psi(x)$ creates a $5 \otimes 5$ or 0-link pion.

Other naive-quark operators can be recast in terms of the spinor/taste operators. For example, the naive-quark action has a chiral symmetry in the massless limit under transformations

$$\begin{aligned} \psi(x) &\to \exp(i\theta\gamma_5 \otimes \xi_5)\psi(x), \\ \bar{\psi}(x) &\to \bar{\psi}(x)\exp(i\theta\gamma_5 \otimes \xi_5), \end{aligned} \tag{E17}$$

where the $\xi_5$s express the fact that the symmetry operation does not translate (move) $\psi(x)$.

## APPENDIX F: ONE-LOOP TASTE CHANGING

The Symanzik procedure for removing $\mathcal{O}(a^2)$ one-loop taste-exchange effects from the ASQTAD action involves two steps: (1) we compute taste-changing amplitudes for $q\bar{q} \to q\bar{q}$ with massless quarks in one-loop order using lattice perturbation theory; and (2) we design local taste-changing counterterms for the staggered-quark action that cancel these one-loop amplitudes. We find it easiest to work with the naive-quark theory, converting to staggered quarks only at the end.

In order $a^2$ we need only consider quarks at threshold—that is, quarks with momentum $p = \pm\zeta\pi$ for one of the 16 $\zeta$'s with $\zeta_\mu \in \mathbb{Z}_2$ (where, again, $a = 1$). Taste-changing amplitudes are ones where the incoming and outgoing momenta along any particular quark line differ by $\zeta\pi$ for one of the $\zeta$s. For $q\bar{q} \to q\bar{q}$, overall momentum conservation demands that the opposite change occur along the other quark line. Consequently while taste changes along individual quark lines, total taste is conserved. It is enough to compute amplitudes $A(0, 0; \zeta\pi, -\zeta\pi)$ where the initial quarks have zero momentum and the final quarks have momenta $\zeta\pi$ for any $\zeta$. (Recall that $\zeta\pi$ and $-\zeta\pi$ are the same momentum on the lattice.) Amplitudes with other quark tastes in the initial state are related to these amplitudes by applying the doubling symmetry to each quark line separately:

$$A(\zeta'\pi, \zeta''\pi; (\zeta' + \zeta)\pi, (\zeta'' - \zeta)\pi) = A(0, 0; \zeta\pi, -\zeta\pi), \tag{F1}$$

where $\zeta'_\mu, \zeta''_\mu \in \mathbb{Z}_2$.

Tree-level contributions come from Fig. 1, but these vanish (by design) in the ASQTAD action because of ASQTAD's quark-gluon vertex. The only one-loop contributions that are nonzero are those shown in Fig. 3; all other one-loop amplitudes have at least one quark line with only one gluon attached, and these vanish, again, because of ASQTAD's quark-gluon vertex. The internal quarks and gluons in the remaining diagrams are all highly virtual, and therefore these contributions can be canceled by a sum of four-quark counterterms each consisting of a product of two quark bilinears (with one bilinear per quark line).

The types of quark bilinear that can arise from these diagrams are greatly restricted by color conservation, chiral symmetry, and the doubling symmetry of the Lagrangian. Quark bilinears can only carry singlet or octet color: thus color structure is either $\bar{\psi}\psi$ or $\bar{\psi}T^a\psi$ where $T^a$ is an $SU(3)$ generator in the fundamental representation. The standard chiral symmetry of the naive-quark action in the massless limit implies that only vector and axial-vector bilinears can arise in that limit: thus spinor structure is either $\bar{\psi}\gamma_\mu\psi$ or $\bar{\psi}\gamma_{5\mu}\psi$. Finally doubling symmetry (Eq. (F1)) requires that the bilinears in the counterterms must be point-split so that they are invariant under any doubling transformation of their quark fields (Eq. (6)): that is, we have

$$\bar{\psi}(x)\gamma_n\psi(x + \delta x(n)) \tag{F2}$$

or

$$\bar{\psi}(x)\gamma_n T^a\psi(x + \delta x(n)), \tag{F3}$$

where $n$ is $\mu$ or $5\mu$, and $\delta x(n)$ is chosen to make the bilinear invariant under $\psi \to \mathcal{B}_\zeta\psi$ for all $\zeta$. This last restriction implies that the bilinears must be staggered-quark operators $\mathcal{J}_n^{(s)}$, as defined in Appendix F.

The one-loop amplitude, $A(0, 0; \zeta\pi, -\zeta\pi)$, for a given $\zeta$ is canceled by a specific set of counterterms,

$$\frac{1}{2}\sum_n d_n^{(s)}|\mathcal{J}_n^{(s)}|^2 + \text{color octet version}, \tag{F4}$$

where $s = \bar{\zeta}$ (from Eq. (E2)). Consider, for example, the case where $\zeta_\mu = 1$ for some $\mu$ while $\zeta_\nu = 0$ for all $\nu \neq \mu$. The taste is $s = \bar{\zeta}$ or $5\mu$. The spin $n$ depends upon the spinor structure of $A$. For this $\zeta$ there are four different spinor structures, each corresponding to a different staggered-quark operator:

$$\begin{aligned} &(\bar{\psi}\gamma_\mu\psi)^2 \to (\mathcal{J}_5^{(5\mu)})^2, \qquad (\bar{\psi}\gamma_\nu\psi)^2 \to (\mathcal{J}_{5\nu\mu}^{(5\mu)})^2, \\ &(\bar{\psi}\gamma_{5\mu}\psi)^2 \to (\mathcal{J}_1^{(5\mu)})^2, \qquad (\bar{\psi}\gamma_{5\nu}\psi)^2 \to (\mathcal{J}_{\mu\nu}^{(5\mu)})^2. \end{aligned} \tag{F5}$$

Each of these operators comes in color octet and color singlet versions, so eight counterterms are required to cancel $A$ for $\zeta^2 = 1$.

The coefficients $d_n^{(s)}$ in the counterterms are computed by on-shell matching of the scattering amplitude $A(0, 0; \zeta\pi, -\zeta\pi)$ to the sum of counterterms for each $\zeta$. Our results are summarized in Table II. Only the bilinears shown in Eq. (33) are needed here. The chiral perturbation theory devised by Lee and Sharpe [35] has ten additional bilinears, but eight of these are not invariant under doubling transformations for each quark line *separately*, and two do not involve taste exchange.

## APPENDIX G: MESON PROPAGATORS

The fact that the single naive-quark field encodes 16 different, identical tastes of quark has practical implications for simulations. For example, the operator

$$J_5(x) \equiv \bar{\psi}(x)\gamma_5\Psi_b(x), \tag{G1}$$

where $\Psi_b$ is an unstaggered $b$-quark field and $\psi$ is a light-quark field, couples only to $J^P = 0^-$ mesons in the continuum, including the $B$. If $\psi$ is a staggered field, however, it also couples to $0^+$ mesons [36].

The doubling-symmetry formula, Eq. (6), is useful in decoding such situations. The second contribution from $J_5$ arises from high-energy states that couple to it. In simulations one normally forms correlators like

$$G_{55}(t) \equiv \sum_{\mathbf{x}}\langle 0|J_5(\mathbf{x}, t)J_5^\dagger(0, 0)|0\rangle, \tag{G2}$$

where the sum over $\mathbf{x}$ guarantees that total three momentum $\mathbf{p} = 0$. The operators, however, are not smeared in time, and so can create arbitrarily high-energy states. The $b$-quark resists large energies, as these drive it far off shell, but the staggered quark is on shell when its energy $E \approx 0$ or when $E \approx \pi$. These two possible states of the light quark correspond to two different tastes. Consequently $J_5$ couples to two different mesons: one whose light quark has taste $\zeta = 0$, and one whose light quark has taste $\zeta = (1, 0, 0, 0)$ or $E \approx \pi$.

The first of these two meson states is the normal $0^-$ $B$ meson. To interpret the second state, we transform the high-energy staggered-quark field back to a low-energy field (which we understand, since it behaves normally) using the doubling-symmetry formula, Eq. (6):

$$\bar{\psi}(x)|_{E\approx\pi} \rightarrow \bar{\psi}(x)(i\gamma_5\gamma_0)(-1)^t. \tag{G3}$$

Substituting in $J_5$ we see that this component of the operator is

$$\bar{\psi}\gamma_5\Psi_b|_{E\approx\pi} \rightarrow \bar{\psi}(i\gamma_5\gamma_0)\gamma_5\Psi_b(-1)^t = -\bar{\psi}i\gamma_0\Psi_b(-1)^t. \tag{G4}$$

The operator $\bar{\psi}i\gamma_0\Psi_b$, now with low-energy fields, couples to $0^+$ mesons. (It is $J = 0$ because there is no three-vector index. It is $P = +$ because $\mathrm{P}\gamma_0\mathrm{P} = \gamma_0$ where $\mathrm{P} \equiv \gamma_0$ is the parity operator.) The full correlator has two components:

$$G_{55}(t) \rightarrow |\langle 0|\bar{\psi}\gamma_5\Psi_b|0^-\rangle|^2 \mathrm{e}^{-E_- t} - (-1)^t|\langle 0|\bar{\psi}i\gamma_0\Psi_b|0^+\rangle|^2\mathrm{e}^{-E_+ t}. \tag{G5}$$

The second component, rather unconventionally, oscillates in sign from time step to time step.


[1] C. T. H. Davies *et al.* (HPQCD Collaboration, Fermilab Collaboration, MILC Collaboration, and UKQCD Collaboration), Phys. Rev. Lett. **92**, 022001 (2004).

[2] C. Aubin *et al.* (MILC Collaboration), Phys. Rev. D **70**, 114501 (2004).

[3] Q. Mason *et al.* (HPQCD Collaboration), Phys. Rev. Lett. **95**, 052002 (2005).

[4] C. Aubin *et al.*, Phys. Rev. Lett. **95**, 122002 (2005).

[5] Q. Mason, H. D. Trottier, R. Horgan, C. T. H. Davies, and G. P. Lepage (HPQCD Collaboration), Phys. Rev. D **73**, 114501 (2006).

[6] S. Naik, Nucl. Phys. **B316**, 238 (1989).

[7] D. Toussaint and K. Orginos (MILC Collaboration), Nucl. Phys. B, Proc. Suppl. **73**, 909 (1999); Phys. Rev. D **59**, 014501 (1998).

[8] G. P. Lepage, Nucl. Phys. B, Proc. Suppl. **60**, 267 (1998).

[9] J. F. Lagae and D. K. Sinclair, Nucl. Phys. B, Proc. Suppl. **63**, 892 (1998); Phys. Rev. D **59**, 014511 (1998).

[10] G. P. Lepage, Phys. Rev. D **59**, 074502 (1999).

[11] A. Hasenfratz and F. Knechtli, Phys. Rev. D **64**, 034504 (2001).

[12] See, for example, A. Gray, I. Allison, C. T. H. Davies, E. Gulez, G. P. Lepage, J. Shigemitsu, and M. Wingate (HPQCD Collaboration and UKQCD Collaboration), Phys. Rev. D **72**, 094507 (2005).

[13] See, for example: C. Bernard, M. Golterman, and Y. Shamir, hep-lat/0610003; M. Creutz, hep-lat/0608020; Y. Shamir, hep-lat/0607007; C. Bernard, M. Golterman, Y. Shamir, and S. R. Sharpe, hep-lat/0603027; M. Creutz, hep-lat/0603020.

[14] S. Sharpe, Proc. Sci. LAT2006 (2006) 022 [hep-lat/0610094].

[15] C. R. Allton *et al.* (UKQCD Collaboration), Phys. Rev. D **65**, 054502 (2002).

[16] See, for example, C. Aubin *et al.*, Phys. Rev. D **70**, 094505 (2004); C. Aubin *et al.* (MILC Collaboration), Nucl. Phys. B, Proc. Suppl. **129**, 227 (2004).

[17] The requirement $m > 0$ is necessary so that $|\det(\mathcal{D})| = \det(\mathcal{D}(U)) > 0$. The naive-quark theory does *not* give correct results when $m < 0$ since then $\det(D \cdot \gamma + m)$ can be negative (if instantons are present). Fortunately the masses of real quarks are not negative. Creutz has suggested that the exact $m \rightarrow -m$ symmetry of this theory might lead to problems for small positive quark masses as well, but the issue he raises is resolved by Bernard *et al.* and does not lead to problems for any $m > 0$ provided the continuum limit is taken before the chiral limit [13,14].

[18] C. Aubin and C. Bernard, Phys. Rev. D **73**, 014515 (2006).

[19] E. Follana, A. Hart, C. T. H. Davies, and Q. Mason (HPQCD Collaboration), Phys. Rev. D **72**, 054501 (2005); E. Follana, A. Hart, and C. T. H. Davies (HPQCD Collaboration), Phys. Rev. Lett. **93**, 241601 (2004).See also, K. Y. Wong and R. M. Woloshyn, Phys. Rev. D **71**, 094508 (2005); S. Durr and C. Hoelbling, Phys. Rev. D **71**, 054501 (2005); S. Durr, C. Hoelbling, and U. Wenger, Phys. Rev. D **70**, 094502 (2004); S. Durr and C. Hoelbling, Phys. Rev. D **69**, 034503 (2004).

[20] Specifically, the minimum mass is related to the eigenvalues which correspond in the continuum to zero modes caused by instantons. In our lattice formalisms these eigenvalues are $\mathcal{O}(a^2)$, and so are small rather than zero [19]. It is important that quark masses be kept significantly larger than these eigenvalues in order to capture instanton effects accurately; for a detailed discussion see [14] and references therein.

[21] Tadpole improvement requires dividing every $U_\mu$ in the final action by a mean link factor $u_0$ (after expanding products of operators so as to remove factors of $U_\nu(x)^\dagger U_\nu(x) = 1$); see G. P. Lepage and P. B. Mackenzie, Phys. Rev. D **48**, 2250 (1993).

[22] G. P. Lepage, Nucl. Phys. B, Proc. Suppl. **26**, 45 (1992).

[23] G. P. Lepage, "," in Proceedings of the 35th International School on Nuclear and Particle Physics, Schladming, Austria, 1996 (to be published), hep-lat/9607076.

[24] Q. J. Mason, Ph.D. Thesis, Cornell University [Institution Report No. UMI-31-14569, 2004 (unpublished)].
[25] See, for example, Fig. 2 in [1] where the upper line in each pair of closely spaced lines comes from a simulation with twice the $u/d$ sea-quark mass.
[26] S. Aoki *et al.*, Nucl. Phys. B, Proc. Suppl. **42**, 303 (1995).
[27] W.-M. Yao *et al.* (Particle Data Group), J. Phys. G **33**, 1 (2006).
[28] G. T. Bodwin, E. Braaten, and G. P. Lepage, Phys. Rev. D **51**, 1125 (1995); **55**, 5853 (1997).
[29] The perturbative result for a $\eta_c$ is the same, up to an overall factor, as for parapositronium. See, for example, G. Adkins in *Relativistic, Quantum Electrodynamic and Weak Interaction Effects in Atoms*, edited by W. Johnson *et al.*, AIP Conf. Proc. No. 189 (AIP, New York, 1989).
[30] E. Follana, Q. Mason, C. Davies, K. Hornbostel, P. Lepage, and H. Trottier (HPQCD Collaboration), Nucl. Phys. B, Proc. Suppl. **129**, 447 (2004).
[31] W. Kamleh, D. B. Leinweber, and A. G. Williams, Phys. Rev. D **70**, 014502 (2004).
[32] C. Morningstar and M. J. Peardon, Phys. Rev. D **69**, 054501 (2004).
[33] See, for example, Section 4.3 in I. Montvay and G. Munster, *Quantum Fields on a Lattice* (Cambridge University Press, Cambridge, England, 1994); also Section 4.5 in H. J. Rothe, World Sci. Lect. Notes Phys. **59**, 1 (1997).
[34] For a similar argument, applied to staggered quarks directly, see S. R. Sharpe, Nucl. Phys. B, Proc. Suppl. **34**, 403 (1994); S. R. Sharpe, hep-ph/9412243. One could easily design a different blocking scheme that suppressed other tastes up to order $a^2$ or $a^3$ corrections by averaging appropriately over larger lattice volumes than $2^4$ hypercubes. The actions for these new blocked fields would then have $a^2$ or $a^3$ taste violations, respectively. Obviously such errors cannot be fundamental since the underlying equations are the same in each case. Indeed by smearing appropriately over the entire lattice volume, all $a^n$ errors of this sort can be removed:, for example, we can do this by using Fourier transforms to isolate different corners of the Brillouin zone exactly rather than approximately.
[35] W. Lee and S. R. Sharpe, Phys. Rev. D **66**, 114501 (2002).
[36] M. Wingate, J. Shigemitsu, C. T. H. Davies, G. P. Lepage, and H. Trottier, Phys. Rev. D **67**, 054505 (2003).